

# Liquid-liquid phase separation and viscosity within secondary organic aerosol generated from diesel fuel vapors

Mijung Song<sup>1,2</sup>, Adrian M. Maclean<sup>2</sup>, Yuanzhou Huang<sup>2</sup>, Natalie R. Smith<sup>3</sup>, Sandra L. Blair<sup>3</sup>, Julia Laskin<sup>4</sup>, Alexander Laskin<sup>4</sup>, Wing-Sy Wong DeRieux<sup>3</sup>, Ying Li<sup>3</sup>, Manabu Shiraiwa<sup>3</sup>, Sergey A. Nizkorodov<sup>3</sup>, Allan K. Bertram<sup>2\*</sup>

[1] {Department of Earth and Environmental Sciences, Chonbuk National University, Jeollabuk-do, 54896, Republic of Korea}

[2] {Department of Chemistry, University of British Columbia, Vancouver, BC, V6T 1Z1, Canada}

[3] {Department of Chemistry, University of California Irvine, Irvine, CA 92697, USA}

[4] {Department of Chemistry, Purdue University, West Lafayette, IN 47907, USA}

## Abstract

Information on liquid-liquid phase separation (LLPS) and viscosity (or diffusion) within secondary organic aerosol (SOA) is needed to improve predictions of particle size, mass, reactivity, and cloud nucleating properties in the atmosphere. Here we report on LLPS and viscosities within SOA generated by the photooxidation of diesel fuel vapors. Diesel fuel contains a wide range of volatile organic compounds, and SOA generated by the photooxidation of diesel fuel vapors may be a good proxy for SOA from anthropogenic emissions. In our experiments, LLPS occurred over the relative humidity (RH) range of ~70 % to ~100 %, resulting in an organic-rich outer phase and a water-rich inner phase. These results may have implications for predicting the cloud nucleating properties of anthropogenic SOA since the presence of an organic-rich outer phase at high RH values can lower the supersaturation with respect to water required for cloud droplet formation. At  $\leq 10$  % RH, the viscosity was  $\geq 1 \times 10^8$  Pa s, which corresponds to roughly the viscosity of tar pitch. At 38 - 50 % RH the viscosity was in the range of  $1 \times 10^8$  -  $3 \times 10^5$  Pa s. These measured viscosities are consistent with predictions based on oxygen to carbon elemental ratio (O:C) and molar mass as well as predictions based on the number of carbon, hydrogen, and oxygen atoms. Based on the measured viscosities and the Stokes-Einstein relation, at  $\leq 10$  % RH diffusion coefficients of organics within diesel fuel SOA is  $\leq 5.4 \times 10^{-17}$  cm<sup>2</sup> s<sup>-1</sup> and the mixing time of organics within

1 200 nm diesel fuel SOA particles ( $\tau_{mixing}$ ) is  $\geq$  50 h. These small diffusion coefficients and large  
2 mixing times may be important in laboratory experiments, where SOA is often generated and  
3 studied using low RH conditions and on time scales of minutes to hours. At 38 - 50 % RH, the  
4 calculated organic diffusion coefficients are in the range of  $5.4 \times 10^{-17}$  to  $1.8 \times 10^{-13}$  cm<sup>2</sup> s<sup>-1</sup> and  
5 calculated  $\tau_{mixing}$  values are in the range of ~0.01 h to ~50 h. These values provide important  
6 constraints for the physicochemical properties of anthropogenic SOA.

## 7 8 **1 Introduction**

9 Volatile organic compounds (VOCs) are emitted into the atmosphere from both biogenic and  
10 anthropogenic sources (Kanakidou et al., 2005; Hallquist et al., 2009). These VOCs can be  
11 oxidized in the atmosphere, and the oxidized products can form secondary organic aerosol  
12 (SOA) (Hallquist et al., 2009; Ervens et al., 2011). SOA accounts for 20 – 80 % of the mass of  
13 atmospheric aerosol particles (Zhang et al., 2007; Jimenez et al., 2009) and plays an important  
14 role in climate, air quality, and public health (Kanakidou et al., 2005; Jang et al., 2006; Solomon,  
15 2007; Baltensperger et al., 2008; Murray et al., 2010; Wang et al., 2012; Pöschl and Shiraiwa,  
16 2015; Shiraiwa et al., 2017; Shrivastava et al., 2017). Despite the importance of SOA, many of  
17 the physicochemical properties of SOA remain poorly understood.

18 One physicochemical property of SOA that remains insufficiently understood is liquid-liquid  
19 phase separation (LLPS) (Pankow, 2003; Marcolli and Krieger, 2006; Ciobanu et al., 2009;  
20 Bertram et al., 2011; Krieger et al., 2012; Song et al., 2012a; Zuend and Seinfeld, 2012; Veghte  
21 et al., 2013; You et al., 2014; O'Brien et al., 2015; Freedman, 2017). Very recent work has  
22 shown that SOA particles free of inorganic salts can undergo LLPS at a high relative humidity  
23 (RH) with implications for predicting the cloud nucleating properties of SOA (Petters et al.,  
24 2006; Hodas et al., 2016; Renbaum-Wolff et al., 2016; Ovadnevaite et al., 2017; Rastak et al.,  
25 2017; Song et al., 2017; Altaft et al., 2018; Liu et al., 2018; Song et al., 2018; Davies et al.,  
26 2019; Ham et al., 2019). Several of these recent studies investigated SOA generated from a  
27 single VOC (e.g.,  $\alpha$ -pinene or isoprene). However, in the atmosphere, SOA is formed from a  
28 complex mixture of VOCs (Odum et al., 1997; Schauer et al., 2002a; 2002b; Vutukuru et al.,  
29 2006; Velasco et al., 2007; de Gouw et al., 2008; Velasco et al., 2009; Gentner et al., 2012; Liu  
30 et al., 2012; Hayes et al., 2015). Additional studies are needed to determine if SOA generated  
31 from a complex mixture of VOCs of atmospheric relevance can also undergo LLPS at high RH.

1 Another physicochemical property of SOA that remains poorly understood is viscosity.  
2 Viscosity together with the Stokes-Einstein equation can be used to predict diffusion rates of  
3 organics within SOA, which can critically impact a number of processes involving SOA. For  
4 example, diffusion of organics within SOA can impact particle size distributions (Shiraiwa et  
5 al., 2013a; Zaveri et al., 2014; Zaveri et al., 2018) and particle mass concentrations (Shiraiwa  
6 and Seinfeld, 2012; Ye et al., 2016; Yli-Juuti et al., 2017; Kim et al., 2019) in the atmosphere.  
7 Diffusion rates within SOA can also affect multi-phase reactions (Shiraiwa et al., 2011; Zhou  
8 et al., 2013; Steimer et al., 2014; Houle et al., 2015; Li et al., 2018), the extent of long-range  
9 transport of pollutants (Zelenyuk et al., 2012; Zhou et al., 2013; Shrivastava et al., 2017; Mu  
10 et al., 2018), ice nucleation (Murray et al., 2010; Wang et al., 2012; Wilson et al., 2012; Ladino  
11 et al., 2014; Schill et al., 2014; Knopf et al., 2018), and crystalline of salts (Murray, 2008;  
12 Murray and Bertram, 2008; Bodsworth et al., 2010; Song et al., 2013; Ji et al., 2017; Wang et  
13 al., 2017).

14 Recently, a number of studies have investigated viscosity or diffusion rates within SOA  
15 particles generated in the laboratory (Virtanen et al., 2010; Cappa et al., 2011; Perraud et al.,  
16 2012; Saukko et al., 2012; Abramson et al., 2013; Robinson et al., 2013; Renbaum-Wolff et al.,  
17 2013; Loza et al., 2013; Kidd et al., 2014; Pajunoja et al., 2014; Bateman et al., 2015; Li et al.,  
18 2015; Song et al., 2015; Wang et al., 2015; Zhang et al., 2015; Grayson et al., 2016; Liu et al.,  
19 2016; Song et al., 2016a; Ye et al., 2018; Ullmann et al., 2019). Almost all of these studies  
20 focused on SOA generated from a single VOC. Additional studies that quantify the viscosity  
21 of SOA generated from a complex mixture of VOCs of atmospheric relevance are also needed.  
22 Functional group contribution methods have recently been used to predict viscosities within  
23 organic matrices of atmospheric relevance (Song et al., 2016a; Song et al., 2016b; Grayson et  
24 al., 2017; Rothfuss and Petters, 2017). Methods have also been developed to predict the glass  
25 transition temperature and viscosity within an organic matrix of atmospheric relevance using  
26 molar mass and oxygen to carbon elemental ratio (O:C) (Shiraiwa et al., 2017) or the number  
27 of carbon, hydrogen, and oxygen atoms of the organic compounds within the organic matrix  
28 (DeRieux et al., 2018). These methods, if accurate, should be useful for predicting viscosity of  
29 SOA particles in the atmosphere.

30 Diesel fuel contains a wide range of VOCs including aromatics and alkanes. Furthermore, SOA  
31 generated from the photooxidation of diesel fuel vapors may be a good proxy for SOA from  
32 anthropogenic emissions (Odum et al., 1997; Schauer et al., 2002a; 2002b; Vutukuru et al.,

1 2006; Velasco et al., 2007; Velasco et al., 2009; de Gouw et al., 2008; Gentner et al., 2012; Liu  
2 et al., 2012; Jathar et al., 2013; Jathar et al., 2014; Hayes et al., 2015; Blair et al., 2017; Gentner  
3 et al., 2017; Jathar et al., 2017). In this study, we investigate LLPS and viscosity within SOA  
4 particles generated by photooxidation of diesel fuel vapors. Measured viscosities are also  
5 compared with predicted viscosities based on the methods developed by Shiraiwa et al. (2017)  
6 and DeRieux et al. (2018). Based on the measured viscosities and the Stokes-Einstein relation,  
7 diffusion coefficients and mixing times of large organic molecules within diesel fuel SOA were  
8 also estimated.

## 9 10 **2 Experimental**

### 11 **2.1 SOA generation**

12 SOA from the photooxidation of diesel fuel vapors was produced in an identical manner to that  
13 described previously (DSL/NO<sub>x</sub> in Table 1 of Blair et al. (2017)). 45 μL of H<sub>2</sub>O<sub>2</sub> (30 wt %) was  
14 evaporated in a 5.6 m<sup>3</sup> inflatable Teflon chamber to achieve a mixing ratio of 2 parts per million  
15 by volume (ppmv). A mixture of NO in N<sub>2</sub> was injected from a gas cylinder to achieve 0.26  
16 ppmv of NO in the chamber. A volume of 200 μL of Fluka. No. 2 diesel (UST-148, 50 mg mL<sup>-1</sup>  
17 solution of diesel in dichloromethane) was evaporated in the chamber, resulting in a  
18 concentration of 1.8 mg m<sup>-3</sup> organic vapor from diesel and a mixing ratio of 0.22 ppmv (based  
19 on an average molecular weight of 200 g mol<sup>-1</sup> (Blair et al., 2017) and assuming no wall loss).  
20 No seed aerosol was used, and the chamber RH was below 2%. UV-B lamps (FS40T12/UVB,  
21 Solarc Systems Inc.) were used to drive the photooxidation, which lasted for 3 h, followed by  
22 particle collection. After 3 h of photooxidation, the particle mass loading in the chamber was  
23 550 μg m<sup>-3</sup> based on measurements with a scanning mobility particle sizer (SMPS; TSI 3080  
24 Electrostatic Classifier and TSI 3775 Condensation Particle Counter). An Aerodyne time-of-  
25 flight aerosol mass spectrometer (ToF-AMS) was used to measure the particle mass spectra in  
26 V mode. ToF-AMS data was analyzed using Squirrel version 1.61. For elemental analysis we  
27 relied on the improved-ambient method by Canagaratna et al. (2015). Figure S1 shows typical  
28 particle number concentration, mass concentration, and average atomic ratios during the  
29 photooxidation. The O:C values (0.4 to 0.5) were consistent with O:C values reported by Blair  
30 et al. (2017) for identically prepared samples.

31 For the LLPS and viscosity measurements, the SOA from the chamber was collected on  
32 hydrophobic glass slides (12 mm coverslips, Hampton Research, Canada) for 120 min using

1 an inertial impactor. To make the surface of the glass slides hydrophobic, they were coated with  
2 trichloro(1*H*,1*H*,2*H*,2*H*-perfluorooctyl)silane (Sigma-Aldrich) following the procedure  
3 reported in Knopf (2003). After collection, the sizes of the SOA particles on the hydrophobic  
4 glass slides were > 10  $\mu\text{m}$ . These large sizes were formed by impaction and coagulation of the  
5 SOA during collection.

## 6 7 **2.2. Measurements of LLPS**

8 SOA was collected on hydrophobic glass slides by impaction, resulting in SOA particles on the  
9 hydrophobic glass slides with diameters > 10  $\mu\text{m}$  and a spherical cap geometry. LLPS was  
10 detected using an optical microscope (Zeiss Epiplan 10X/0.20 HD) coupled to a flow-cell with  
11 temperature and RH control (Parsons et al., 2004; Pant et al., 2006; Song et al., 2012b). During  
12 the experiments, a constant flow (1.5 L  $\text{min}^{-1}$ ) of humidified  $\text{N}_2$  gas was maintained within the  
13 flow-cell and measured with a dew point hygrometer (General Eastern M4/E4 Dew Point  
14 Monitor, Canada). The temperature within the flow-cell was maintained at  $290 \pm 1$  K and  
15 measured with a thermocouple (OMEGA, Canada). At the beginning of the experiments, the  
16 SOA particles were equilibrated at around 100 % RH for at least 15 min. At this point, the focus  
17 of the microscope was adjusted so the focal plane of the microscope corresponded to the top  
18 or interior of several SOA particles. Due to the different sizes of the SOA particles on the  
19 hydrophobic glass slides, the focal plane of the microscope corresponded to the top of some  
20 SOA particles and the middle of some SOA particles while some smaller particles were not in  
21 the focal plane (leading to blurry images). Next, the RH was reduced at a rate of 0.5% RH  $\text{min}^{-1}$   
22 until a value close to 0% was reached. While the RH was decreased, images of the particles  
23 were acquired every 10 sec with a CCD camera connected to the microscope. From the images,  
24 the number of phases (e.g. one phase or two phases) present in the particles were determined.  
25 Typically the focus of the microscope was not adjusted as the RH was reduced. As the RH was  
26 reduced, the size of the SOA particles decreased due to the loss of water, and some SOA  
27 particles that were in focus at high RH values became out of focus at low RH values.

## 28 29 **2.3 Measurements of particle viscosity**

30 The viscosity of the collected particles was determined using the poke-and-flow technique,  
31 which has been described by Renbaum-Wolff et al. (2013) and Grayson et al. (2015), and based,  
32 in part, on the earlier experiments by Murray et al. (2012). In short, the SOA particles collected

1 on hydrophobic glass slides were placed inside a flow-cell with RH and temperature control  
2 (Pant et al., 2006; Bertram et al., 2011; Song et al., 2012a). After conditioning the particles to  
3 a known RH at  $294 \pm 1$  K, the particles were poked with a sharp needle ( $\sim 10$   $\mu\text{m}$  for the tip of  
4 the needle) (Becton-Dickson, USA). The movement of the needle was controlled with a  
5 micromanipulator (Narishige, model MO-202U, Japan). The change in morphology as a  
6 function of time after poking the particles with the needle was recorded with a camera attached  
7 to the microscope. From the morphology changes and fluid dynamics simulations, upper and  
8 lower limits to the SOA viscosity were determined. Fluid dynamics simulations were  
9 performed using the finite-element analysis software package, *COMSOL Multiphysics*  
10 (Renbaum-Wolff et al., 2013; Grayson et al., 2015). The geometry used in the simulations was  
11 based on the geometry of the particles after poking them with a needle. Additional details of  
12 the poke-and-flow experiments and the fluid dynamics simulations are discussed in Sect. 3.2  
13 and Sect. S1-S3 of the Supplement.

14 In the poke-and-flow experiments (as well as the LLPS experiments), the particles are exposed  
15 to a constant flow of gas which can lead to a change in the composition of the particles by  
16 partitioning of semi-volatiles to the gas phase. For a 1 hr poke-and-flow experiment, the  
17 amount of gas exposed to the SOA is 30 L compared to 380 L collected from the environmental  
18 chamber. Exposing the SOA to this amount of gas can be considered equivalent to changing  
19 the mass loading used to generate the SOA from  $550 \mu\text{g m}^{-3}$  to  $510 \mu\text{g m}^{-3}$ . Exposing the  
20 particles to a constant gas flow for 27 hours (maximum amount of time a sample was exposed  
21 to a constant gas flow) can be considered equivalent to changing the mass loading from  $550 \mu\text{g m}^{-3}$   
22 to  $175 \mu\text{g m}^{-3}$ . This should be considered a worse-case scenario since this estimation does  
23 not consider kinetic constraints to evaporation. Based on previous measurements, the viscosity  
24 of toluene SOA is independent of mass loadings ranging from  $\sim 800 \mu\text{g m}^{-3}$  to  $\sim 80 \mu\text{g m}^{-3}$  (Song  
25 et al., 2016a). Assuming that diesel fuel SOA behaves like toluene SOA, the viscosity of diesel  
26 fuel SOA should not be influenced by exposure to a constant flow of gas in our poke-and-flow  
27 experiments. Consistent with this discussion, we did not observe a relationship between particle  
28 viscosity and time the SOA was exposed to a constant flow of gas in our experiments.

29

## 30 **2.4 Predictions of viscosity based on high-resolution mass spectrometry**

31 Viscosities of the diesel fuel SOA was predicted using the elemental composition of the SOA  
32 and the methods developed by Shiraiwa et al. (2017) and DeRieux et al. (2018). The elemental

1 compositions of the diesel fuel SOA were taken from a previous study (Blair et al., 2017) using  
2 of SOA generated with identical conditions (DSL/NO<sub>x</sub> Table 1 of Blair et al. (2017)). In the  
3 previous study by Blair et al. (2017) high-resolution nanospray desorption electrospray  
4 ionization mass spectrometry (Roach et al., 2010) was used to determine the elemental  
5 composition.

6 Shiraiwa et al. (2017) reported a parameterization (Eq. 1) to estimate the glass transition  
7 temperature ( $T_g$ ) of individual CH or CHO compounds with molar mass  $< \sim 450 \text{ g mol}^{-1}$ .

8

$$9 \quad T_g = A + BM + CM^2 + D (\text{O:C}) + E M (\text{O:C}) \quad (1)$$

10

11 where  $M$  is the molar mass and O:C is the ratio of oxygen to carbon atoms. The coefficients  
12 are:  $A = -21.57 \text{ (K)}$ ,  $B = 1.51 \text{ (K mol g}^{-1}\text{)}$ ,  $C = -1.7 \times 10^{-3} \text{ (K mol}^2 \text{ g}^{-2}\text{)}$ ,  $D = 131.4 \text{ (K)}$  and  $E = -$   
13  $0.25 \text{ (K mol g}^{-1}\text{)}$ .

14 DeRieux et al. (2018) reported another parameterization (Eq. 2) to predict  $T_g$  of CH and CHO  
15 compounds with molar mass up to  $\sim 1100 \text{ g mol}^{-1}$  using the number of carbon ( $n_C$ ), hydrogen  
16 ( $n_H$ ), and oxygen atoms ( $n_O$ ):

17

$$18 \quad T_g = (n_C^0 + \ln(n_C)) b_C + \ln(n_H) b_H + \ln(n_C) \ln(n_H) b_{CH} + \ln(n_O) b_O + \ln(n_C) \ln(n_O) b_{CO} \quad (2)$$

19

20 Values of the coefficients [ $n_C^0$ ,  $b_C$ ,  $b_H$ ,  $b_{CH}$ ,  $b_O$ , and  $b_{CO}$ ] are [1.96, 61.99, -113.33, 28.74, 0, 0]  
21 for CH compounds and [12.13, 10.95, -41.82, 21.61, 118.96, -24.38] for CHO compounds  
22 (DeRieux et al., 2018).

23 To estimate the  $T_g$  for a dry organic mixture ( $T_{g,\text{org}}$ ), the relative mass concentration of each  
24 compound was assumed to be proportional to its relative abundance in the mass spectrum and  
25 the Gordon-Taylor mixing rule was employed with a Gordon-Taylor coefficient ( $k_{GT}$ ) value of  
26 1, as done previously for organic-organic mixtures (Dette et al., 2014).

27 For the  $T_g$  of a mixture of organics and water ( $T_{g,\text{mix}}$ ), the effective hygroscopicity parameter  
28 ( $\kappa$ ) was applied to calculate the mass fraction of water in the SOA particles (Petters and  
29 Kreidenweis, 2007). A  $\kappa$  value of 0.1 was used for the diesel fuel SOA based on an average  
30 O:C of 0.45 for diesel fuel-derived SOA (Fig.S1 and Table S2 in Blair et al. (2017)) and the  
31 relationship between O:C and  $\kappa$  reported in Lambe et al. (2011, Fig. 7) and Massoli et al. (2010,  
32 Fig. 2). To estimate the  $T_{g,\text{mix}}$ , the Gordon-Taylor equation was applied with  $k_{GT}$  set to 2.5,

1 based on previous studies that suggested  $2.5 \pm 1.0$  for organic-water mixtures (Zobrist et al.,  
2 2008; Koop et al., 2011; Berkemeier et al., 2014).

3 Once  $T_{g,mix}$  was determined, viscosity was estimated using the modified Vogel-Tammann-  
4 Fulcher (VTF) equation and an assumed viscosity of  $10^{12}$  Pa s at the glass transition  
5 temperature ( $T = T_g$ ) and an assumed viscosity of  $10^{-5}$  Pa s at a very high temperature:

$$7 \log \eta = -5 + 0.434 \frac{T_0 D_f}{T - T_0} \quad (3)$$

$$8 \text{ where } T_0 = \frac{39.17 T_g}{D_f + 39.17} \quad (4)$$

9  
10 The viscosity of  $10^{-5}$  Pa s at a very high temperature is well established in the glass community  
11 (Angell, 1991; Angell, 2002). In these equations,  $D_f$  is the fragility parameter and  $T_0$  is the  
12 Vogel temperature. In our calculations, we fixed  $D_f$  to be 10 because a previous study that  
13 showed  $D_f$  approaches 10 when the molar mass of the organic compounds exceed  $\sim 200$  g mol<sup>-1</sup>  
14 (DeRieux et al., 2018) and because many of the detected compounds in diesel SOA have  
15 molar masses  $> 200$  g mol<sup>-1</sup>. Even though the  $D_f$  value does affect predicted viscosity (see Fig.  
16 5b in DeRieux et al., 2018),  $D_f$  is not as critical as other parameters such as the glass transition  
17 temperature or hygroscopicity.

### 19 **3 Results and discussion**

#### 20 **3.1 LLPS in diesel fuel SOA**

21 Figures 1 and S2 show examples of images recorded during the LLPS experiments as the RH  
22 was decreased from  $\sim 100\%$  to  $\sim 0\%$ . **The five particles shown in Figs. 1 and S2 were produced**  
23 **with the same reaction conditions.** At the highest RH values ( $\sim 100\%$ ), two phases were  
24 observed in all cases. The inner phase was most likely a water-rich phase while the outer phase  
25 was likely an organic-rich phase since the inner phase decreased in size as the RH decreased.  
26 This conclusion is consistent with surface tensions of organics and experiments that have  
27 investigated morphology of particles after LLPS (Jasper, 1972; Kwamena et al., 2010; Reid et  
28 al., 2011; Song et al., 2013; O'Brien et al., 2015; Gorkowski et al., 2016, 2017). The organic-  
29 rich phase was most likely non-crystalline since SOA contains thousands of molecules and the  
30 concentration of any individual molecule is likely below the concentration required for



1 crystallization (Marcolli et al., 2004). At ~70 % RH, two liquid phases remained in all particles  
2 (Figs. 1 and S2). Small amounts of the water-rich phase were present even at  $\lesssim$  50 % RH in  
3 most cases (Figs. 1 and S2). In the few cases where LLPS was not observed at  $\lesssim$  50 % RH, two  
4 liquid phases may still have been present in the particles, but not in the focus of the microscope.

5 In the previous studies using SOA derived from a single VOC, LLPS was observed when the  
6 average O:C was between 0.34 and 0.44 but not when the average O:C was between 0.52 and  
7 1.30 (Renbaum-Wolff et al., 2016; Rastak et al., 2017; Song et al., 2017). Consistent with this  
8 trend, in the current studies, we observed LLPS when the O:C values of the SOA was 0.4 - 0.5  
9 (Fig. S1b). However, in the previous studies using SOA derived from a single VOC, LLPS was  
10 only observed between ~95 % and close to ~100 % RH. Whereas, in the current study, LLPS  
11 was observed between ~70 % and close to ~100 %. This suggests that as the complexity of  
12 SOA increases, LLPS can occur over a wider range of RH values. Consistent with this  
13 conclusion, in a recent study, we showed that LLPS in organic particles containing two  
14 commercially available organic compounds occurs over a wider RH range than in particles  
15 containing only one organic compound (Song et al., 2018).

16 The increase in the range of RH values over which LLPS occurs is likely related to distribution  
17 of the polarities (or hydrophilicities) of the organics molecules within the SOA (Renbaum-  
18 Wolff et al., 2016; Gorkowski et al., 2019). When the organic molecules are hydrophobic or  
19 moderately hydrophobic (and hence have small O:C values) the particles are expected to have  
20 a single organic-rich phase until close to 100% RH, at which point LLPS can occur. When the  
21 organic molecules are hydrophilic (and hence have large O:C values), the particles are expected  
22 to have a single water-rich phase, with no occurrence of LLPS. Alternatively, if the particles  
23 contain a mixture of hydrophobic and hydrophilic organic molecules, the particles are expected  
24 to have both an organic-rich phase and a water-rich phase over a relatively wide range of RH  
25 values. A significant amount of molecules with low and high O:C values in the diesel SOA  
26 studied here (Fig. S3) is consistent with LLPS being observed over a relatively wide range of  
27 RH values.

## 28 29 **3.2 Viscosity of diesel fuel-derived SOA**

### 30 **3.2.1 Lower limits to viscosity at 10% RH**

1 In these experiments, the RH was first decreased to 10% and particles were conditioned at this  
2 RH for approximately 1 h. After conditioning, the particles were poked with a needle, which  
3 caused the particles to crack (Fig. 2a). After poking, the sharp edges that resulted from cracking  
4 moved by less than 0.5  $\mu\text{m}$  in 5 h. The distance of 0.5  $\mu\text{m}$  corresponds to the minimum amount  
5 of movement that could be discerned in our microscope setup. Based on these results and fluid  
6 dynamics simulations (Sect. S1 in the Supplement), the lower limit to the viscosity at 10 % RH  
7 is  $1 \times 10^8$  Pa s (Fig. 3a). This corresponds to roughly the viscosity of tar pitch (Koop et al., 2011).

### 8 **3.2.2. Lower limits to viscosity at 31 and 50 % RH**

9 In these experiments, the RH was first decreased to 31 % or 50 %, and conditioned at these RH  
10 values for 1 h and 0.5 h, respectively. After conditioning the particles at either 31 or 50 % RH,  
11 they were poked with a needle, resulting in the formation of a half-torus geometry (Figs. 2b  
12 and 2c). From images recorded after poking the particles, the experimental flow time,  $\tau_{exp, flow}$ ,  
13 was determined, which corresponds to the time for the equivalent-area diameter of the inside  
14 of the half torus geometry to reduce by 50 %. The equivalent-area diameter,  $d$ , was calculated  
15 via the relationship  $d = (4A/\pi)^{1/2}$  where  $A$  is the hole area (Reist, 1992). Based on the measured  
16  $\tau_{exp, flow}$  values and fluid dynamics simulations (Renbaum-Wolff et al., 2013; Grayson et al.,  
17 2015), and Sect. S2 in the Supplement, the lower limit to the viscosity is approximately  $3 \times 10^4$   
18 and  $8 \times 10^5$  Pa s at 50 % and 31 % RH, respectively (Fig. 3a). For reference, the viscosity of  
19 peanut butter corresponds is approximately  $10^3$  Pa s (Koop et al., 2011).

### 20 **3.2.3. Upper limits to viscosity at RH values ranging from 38 to 60 %**

21 In these experiments, the following new procedure was used. First, the particles were exposed  
22 to a dry nitrogen flow at 0 % RH for  $\sim 1$  h. After this exposure, the particles were poked with a  
23 needle resulting in cracking of the particles. The RH above the particles was then increased in  
24 a single step to one of the following RH values: 38 %, 41 %, 48 %, 53 %, 57 %, and 60 %. As  
25 the RH increased and then stabilized (which took 5-10 min), the cracked particles began to  
26 flow and returned to an approximately spherical cap shape (e.g. Fig. 4). From images recorded  
27 during these experiments, the time required for the particles to return to a spherical cap shape  
28 (starting from the cracked particles at RH= 0%) was determined. This time (which included  
29 the time for the RH to increase and stabilize) was referred to as the experimental recovery time,  
30  $\tau_{exp, recovery}$ . Based on the  $\tau_{exp, recovery}$  values and fluid dynamics simulations (Sect. S3 in the  
31 Supplement), the upper limits of the viscosity is  $\sim 1 \times 10^7$  Pa s and  $\sim 1 \times 10^8$  Pa s at RH values of

1 60 % and 38 %, respectively (Fig. 3a).

### 2 **3.2.4 Comparison with previous measurements and predictions**

3 In Fig. 3b the measured viscosities determined from individual poke-and-flow experiments are  
4 grouped by RH and compared with the viscosity of SOA generated by the photooxidation of  
5 toluene. Toluene SOA is commonly used as a proxy of anthropogenic SOA (Pandis et al., 1992;  
6 Robinson et al., 2013; Bateman et al., 2015; Liu et al., 2016; Song et al., 2016). The viscosities  
7 of the toluene SOA and the diesel fuel SOA are similar. At RH values between 38 and 50 %  
8 both have viscosities in the range of approximately  $10^4$  to  $10^8$  Pa s while at  $\leq 10$  % RH, both  
9 have viscosities  $\geq 1 \times 10^8$  Pa s.

10 In Fig. 3b, the viscosity of diesel fuel SOA is also compared with predicted viscosities based  
11 on O:C and molar mass (Eq. 1) and the number of carbon, hydrogen, and oxygen atoms (Eq.  
12 2). Within the uncertainty of the measurements, the predicted viscosities are consistent with  
13 the measured viscosities (Fig. 3b). Measurements of viscosity with reduced uncertainties would  
14 be useful to better test the predictions. Common methods used to measure viscosities (i.e., bulk  
15 viscometers) are more precise than the poke-and-flow technique, but require more material  
16 than is typically produced in environmental chambers (Reid et al., 2018).

17 Interestingly, predictions based on the number of carbon, hydrogen, and oxygen atoms (Eq. 2)  
18 are almost 3 orders of magnitude higher than predictions based on O:C and molar mass (Eq. 1)  
19 for dry conditions (i.e., 0 % RH) (Fig. 3b). Eq. 2 was applied to molar masses up to  $\sim 1100$  g  
20  $\text{mol}^{-1}$  while Eq. 1 was applied to molar masses  $< 450$  g  $\text{mol}^{-1}$ . If Eq. 2 was limited to molar  
21 mass  $< 450$  g  $\text{mol}^{-1}$ , the predicted viscosities would only decrease by a factor of  $\leq 1.3$  (Fig. S6).  
22 The difference in the predictions based on Eq. 2 and Eq. 1 shown in Fig. 3b is due to the  
23 uncertainties in those two parameterizations. More comprehensive experimental  $T_g$  datasets are  
24 needed to further refine the  $T_g$  parameterizations.

25 The predicted viscosities shown in Fig. 3b only consider CH and CHO compounds. For the  
26 diesel fuel SOA studied here, 257 compounds ( $\sim 36\%$  of the intensity weighted peaks) were  
27 CHON compounds (Blair et al., 2017). A comprehensive experimental  $T_g$  dataset for organic  
28 compounds containing nitrogen atoms is required to improve the viscosity predictions of diesel  
29 fuel SOA.

30

### 3.3 Diffusion coefficients and mixing times of large organics within diesel fuel SOA

From the measured viscosities, we calculated diffusion coefficients of the organic molecules within the diesel fuel SOA using the Stokes-Einstein relation:

$$D_{org} = \frac{kT}{6\pi a\eta} \quad (5)$$

Where  $k$  is the Boltzmann constant,  $T$  is the temperature,  $a$  is the hydrodynamic radius of the diffusing species, and  $\eta$  is the dynamic viscosity. To calculate diffusion coefficients, we assumed a hydrodynamic radius of 0.4 nm for the diffusing organic molecules (Renbaum-Wolff et al., 2013). Although the Stokes-Einstein relation may under predict diffusion of small molecules (e.g., OH, O<sub>3</sub>, NO<sub>x</sub>, NH<sub>3</sub>, and H<sub>2</sub>O) in SOA, this equation gives reasonable values when the size of the diffusing organics is similar to the size of the matrix molecules and the temperature is not too close to the  $T_g$  of the matrix (Champion et al., 2000; Marshall et al., 2016; Price et al., 2015, 2016; Bastelberger et al., 2017; Chenyakin et al., 2017; Ullmann et al., 2019). Based on the measured viscosities and the Stokes-Einstein relation, the diffusion coefficients of organics within Diesel SOA is  $\leq 5.4 \times 10^{-17} \text{ cm}^2 \text{ s}^{-1}$  for RH values  $\leq 10\%$  (Fig. 5a, secondary y-axis). For RH values between 38 % and 50 %, the diffusion coefficients are in the range of  $5.4 \times 10^{-17}$  to  $1.8 \times 10^{-13} \text{ cm}^2 \text{ s}^{-1}$ .

From the calculated  $D_{org}$ , the mixing time of organics within 200 nm diesel fuel SOA particles,  $\tau_{mixing}$ , was calculated with the following equation (Seinfeld and Pandis, 2006; Shiraiwa et al., 2011):

$$\tau_{mixing} = \frac{d^2}{4\pi D_{org}} \quad (6)$$

Where  $d$  corresponds to the diameter of the SOA particles. Values of  $\tau_{mixing}$  represent the time after which the concentration of the diffusing molecules at the center of the particles deviates by less than  $e^{-1}$  from the equilibrium concentration. When calculating  $\tau_{mixing}$ , we assumed  $d$  was 200 nm, which is consistent with the median diameter of the volume distribution of SOA in the atmosphere (Martin et al., 2010; Pöschl et al., 2010; Riipinen et al., 2011).

It is often assumed in chemical transport models that organic molecules are well mixed in SOA

1 on the time scale of 1 h. Based on our viscosity results and Eq. 6,  $\tau_{mixing}$  is  $\geq 50$  h at  $\leq 10$  %  
2 RH (Fig. 5a, secondary y-axis). This mixing time is much larger than assumed in chemical  
3 transport models. However, in the planetary boundary layer, the RH is not often  $\leq 10$  %, at  
4 least not when SOA concentrations are significant (Fig. 5b and 5c). Nevertheless, the large  
5  $\tau_{mixing}$  values at  $\leq 10$  % RH, may be important in laboratory experiments, where SOA is often  
6 generated and studied under low RH conditions on the time scales of minutes to hours. **At 38**  
7 **– 50 % RH  $\tau_{mixing}$  are in the range  $\sim 0.01$  h to  $\sim 50$  h (Fig. 5a). These results provide important**  
8 **constraints on  $\tau_{mixing}$  values within anthropogenic SOA.**

9 Several caveats apply to the calculated  $\tau_{mixing}$  values. First, the diesel fuel SOA was generated  
10 using relatively high particle mass concentrations ( $\sim 500 \mu\text{g m}^{-3}$ ). The viscosity of diesel fuel  
11 SOA may be higher if generated using lower particle mass concentrations (Grayson et al., 2016;  
12 Jain et al., 2018). Second,  $\tau_{mixing}$  values may be overestimated at low RH values due to the  
13 possible breakdown of the Stokes-Einstein relation near the glass transition RH (Champion et  
14 al., 2000; Bastelberger et al., 2017; Chenyakin et al., 2017; Evoy et al., 2019; Ullmann et al.,  
15 2019). **Third, when calculating the viscosity, we did not take into account the heterogeneity of**  
16 **the particle (i.e. the presence of both an organic-rich and water-rich phase). The viscosity**  
17 **measurements were carried out at RH values  $\lesssim 58$  % RH. For this RH range, the amount of the**  
18 **water-rich phase was small but still detectable in most cases. Assuming the water-rich phase is**  
19 **less viscous than the organic-rich phase, due to the plasticizing effect of water, the viscosity of**  
20 **the organic-rich phase will be greater than the calculated (i.e. reported) viscosities.**

#### 21 22 **4 Summary and conclusions**

23 We investigated LLPS in SOA generated from diesel fuel vapors. Diesel fuel contains a wide  
24 range of VOCs, and diesel fuel SOA may be a reasonable proxy for SOA from anthropogenic  
25 emissions. Two liquid phases (an organic-rich outer phase and a water-rich inner phase) were  
26 observed in the diesel fuel SOA at RH values ranging from  $\sim 70$  % to  $\sim 100$  %. These results  
27 may be important for predicting the cloud nucleating ability of anthropogenic SOA **since the**  
28 **presence of an organic-rich outer phase at high RH values can lower the supersaturation with**  
29 **respect to water required for cloud droplet formation** (Petters et al. 2006; Hodas et al. 2016;  
30 Renbaum-Wolff et al., 2016; Rastak et al., 2017; Ovadnevaite et al., 2017; Liu et al., 2018).

1 The presence of two liquid phases at RH values as low as ~70 % may also impact heterogeneous  
2 chemistry, growth, and optical properties of SOA (Zuend et al., 2010; Zuend and Seinfeld, 2012;  
3 Shiraiwa et al., 2013b; Freedman, 2017; Fard et al., 2018; Zhang et al., 2018). We conclude  
4 that LLPS should be considered when predicting the cloud nucleating ability, reactivity, growth,  
5 and optical properties of SOA from anthropogenic emissions.

6 We also investigated the viscosity of diesel fuel SOA using the poke-and-flow technique  
7 together with simulations of fluid flow. For RH values of  $\leq 10$  %, the viscosity was  $\geq 1 \times 10^8$  Pa  
8 s. At RH values between 30 and 50 % the viscosity was in the range of  $1 \times 10^8$  to  $3 \times 10^4$  Pa s.  
9 The measured viscosities were consistent with predictions based on molar mass and O:C and  
10 predictions based on the number of carbon, hydrogen, and oxygen atoms of identified SOA  
11 compounds. Additional measurements of viscosity of diesel fuel SOA with reduced  
12 uncertainties would be useful to better test the predictions. Furthermore, additional  
13 comprehensive experimental  $T_g$  datasets are needed to further refine the parameterizations.  
14 Based on these measured viscosities and the Stokes-Einstein relation, diffusion coefficients and  
15  $\tau_{mixing}$  values of organics within diesel fuel SOA particles were calculated. For RH values  $\leq$   
16 10%, diffusion coefficients are  $\leq 5.4 \times 10^{-17}$  cm<sup>2</sup> s<sup>-1</sup> and  $\tau_{mixing}$  is  $\geq 50$  h. Such low RH values  
17 are not common in the planetary boundary layer, but are common in laboratory experiments  
18 when generating SOA. We conclude that these large  $\tau_{mixing}$  should be considered when  
19 interpreting laboratory data of SOA generated under low RH conditions. For RH values  
20 between 38 % and 50 %, the diffusion coefficients are in the range of  $5.4 \times 10^{-17}$  to  $1.8 \times 10^{-13}$   
21 cm<sup>2</sup> s<sup>-1</sup> and  $\tau_{mixing}$  values are in the range of ~0.01 h and ~50 h. These results provide important  
22 constraints on diffusion coefficients and  $\tau_{mixing}$  values within anthropogenic SOA. Further  
23 studies are needed using more atmospherically relevant mass concentrations since a relatively  
24 high mass concentration ( $\sim 500$   $\mu\text{g m}^{-3}$ ) of the SOA was used when generating the SOA in this  
25 work.

26

### 27 **Conflicts of interest**

28 There are no conflicts of interest to declare.

29

### 30 **Author contributions**

31 A.K.B designed the study. M.Song, A.M.M, and Y. H. performed the viscosity and LLPS

1 experiments. S.A.N., N.R.S., S.L.B., J. L., and A.L. generated the SOA samples and analyzed  
2 their chemical compositions. W.-S.W.D., Y.L., and M.S. predicted viscosities. M.Song and  
3 A.K.B. prepared the manuscript with contributions from all co-authors.

#### 4 5 **Acknowledgements**

6 This work was supported by the Natural Sciences and Engineering Research Council of Canada.  
7 M. Song acknowledges funding from the National Research Foundation of Korea (NRF), the  
8 Korea Government (MSIP) (2016R1C1B1009243) and Korea Institute of Toxicology (KIT)  
9 (KK-1905-02). M.S. acknowledges funding from the U.S. National Science Foundation (AGS-  
10 1654104) and the U.S. Department of Energy (DE-SC0018349). The AMS instrument used in  
11 this work was acquired with the NSF grant MRI-0923323.

#### 12 13 **References**

- 14 Abramson, E., Imre, D., Beranek, J., Wilson, J., and Zelenyuk, A.: Experimental determination  
15 of chemical diffusion within secondary organic aerosol particles, *Phys. Chem. Chem.*  
16 *Phys.*, 15, 2983-2991, <https://doi.10.1039/C2cp44013j>, 2013.
- 17 Altaft, M. B., Dutcher, D. D., Raymond, T. M., and Freedman, M. A.: Effect of Particle  
18 Morphology on Cloud Condensation Nuclei Activity, *ACS. Earth Space Chem.*, 2, 634-  
19 639, [10.1021/acsearthspacechem.7b00146](https://doi.10.1021/acsearthspacechem.7b00146), 2018.
- 20 Angell, C. A.: Relaxation in liquids, Polymers and plastic crystals - Strong fragile patterns and  
21 problems, *J. Non-Cryst. Solids*, 131, 13-31, [https://doi.10.1016/0022-3093\(91\)90266-9](https://doi.10.1016/0022-3093(91)90266-9),  
22 1991.
- 23 Angell, C. A.: Liquid fragility and the glass transition in water and aqueous solutions, *Chem.*  
24 *Rev.*, 102, 2627-2649, UNSP CR000689Q [10.1021/cr000689q](https://doi.10.1021/cr000689q), 2002.
- 25 Baltensperger, U., Dommen, J., Alfarra, R., Duplissy, J., Gaeggeler, K., Metzger, A., Facchini,  
26 M. C., Decesari, S., Finessi, E., Reinnig, C., Schott, M., Warnke, J., Hoffmann, T., Klatzer,  
27 B., Puxbaum, H., Geiser, M., Savi, M., Lang, D., Kalberer, M., and Geiser, T.: Combined  
28 determination of the chemical composition and of health effects of secondary organic  
29 aerosols: The POLYSOA project, *J Aerosol Med Pulm D*, 21, 145-154, 2008.
- 30 Bastelberger, S., Krieger, U. K., Luo, B. P., and Peter, T.: Diffusivity measurements of volatile  
31 organics in levitated viscous aerosol particles, *Atmos. Chem. Phys.*, 17, 8453-8471,  
32 [10.5194/acp-17-8453-2017](https://doi.10.5194/acp-17-8453-2017), 2017.

1 Bateman, A. P., Bertram, A. K., and Martin, S. T.: Hygroscopic influence on the semisolid-to-  
2 liquid transition of secondary organic materials, *J. Phys. Chem. A.*, 119, 4386-4395,  
3 10.1021/jp508521c, 2015.

4 Berkemeier, T., Shiraiwa, M., Pöschl, U., and Koop, T.: Competition between water uptake and  
5 ice nucleation by glassy organic aerosol particles, *Atmos. Chem. Phys.*, 14, 12513-12531,  
6 2014.

7 Bertram, A. K., Martin, S. T., Hanna, S. J., Smith, M. L., Bodsworth, A., Chen, Q., Kuwata,  
8 M., Liu, A., You, Y., and Zorn, S. R.: Predicting the relative humidities of LLPS,  
9 efflorescence, and deliquescence of mixed particles of ammonium sulfate, organic material,  
10 and water using the organic-to-sulfate mass ratio of the particle and the oxygen-to-carbon  
11 elemental ratio of the organic component, *Atmos. Chem. Phys.*, 11, 10995-11006,  
12 <https://doi.10.5194/acp-11-10995-2011>, 2011.

13 Blair, S. L., MacMillan, A. C., Drozd, G. T., Goldstein, A. H., Chu, R. K., Pasa-Tolic, L., Shaw,  
14 J. B., Tolic, N., Lin, P., Laskin, J., Laskin, A., and Nizkorodov, S. A.: Molecular  
15 characterization of organosulfur compounds in biodiesel and diesel fuel secondary organic  
16 aerosol, *Environ. Sci. Technol.*, 51, 119-127, 10.1021/acs.est.6b03304, 2017.

17 Bodsworth, A., Zobrist, B., and Bertram, A. K.: Inhibition of efflorescence in mixed organic-  
18 inorganic particles at temperatures less than 250K, *Phys. Chem. Chem. Phys.*, 12, 15144-  
19 15144, 2010.

20 Canagaratna, M. R., Jimenez, J. L., Kroll, J. H., Chen, Q., Kessler, S. H., Massoli, P.,  
21 Hildebrandt Ruiz, L., Fortner, E., Williams, L. R., Wilson, K. R., Surratt, J. D., Donahue,  
22 N. M., Jayne, J. T., and Worsnop, D. R.: Elemental ratio measurements of organic  
23 compounds using aerosol mass spectrometry: characterization, improved calibration, and  
24 implications, *Atmos. Chem. Phys.*, 15, 253-272, 10.5194/acp-15-253-2015, 2015.

25 Cappa, C. D., and Wilson, K. R.: Evolution of organic aerosol mass spectra upon heating:  
26 implications for OA phase and partitioning behavior, *Atmos. Chem. Phys.*, 11, 1895-1911,  
27 <https://doi.10.5194/acp-11-1895-2011>, 2011.

28 Champion, D., Le Meste, M., and Simatos, D.: Towards an improved understanding of glass  
29 transition and relaxations in foods: molecular mobility in the glass transition range, *Trends*  
30 *Food Sci. Tech.*, 11, 41-55, [https://doi.10.1016/S0924-2244\(00\)00047-9](https://doi.10.1016/S0924-2244(00)00047-9), 2000.

31 Chenyakin, Y., Ullmann, D. A., Evoy, E., Renbaum-Wolff, L., Kamal, S., and Bertram, A. K.:  
32 Diffusion coefficients of organic molecules in sucrose-water solutions and comparison



1 with Stokes-Einstein predictions, *Atmos. Chem. Phys.*, 17, 2423-2435, 10.5194/acp-17-  
2 2423-2017, 2017.

3 Ciobanu, V. G., Marcolli, C., Krieger, U. K., Weers, U., and Peter, T.: Liquid-Liquid Phase  
4 Separation in Mixed Organic/Inorganic Aerosol Particles, *J. Phys. Chem. A*, 113, 10966–  
5 10978, <https://doi.org/10.1021/Jp905054d>, 2009.

6 Davies, J. F., Zuend, A., and Wilson, K. R.: Technical note: The role of evolving surface tension  
7 in the formation of cloud droplets, *Atmos. Chem. Phys.*, 19, 2933-2946, 10.5194/acp-19-  
8 2933-2019, 2019.

9 de Gouw, J. A., Brock, C. A., Atlas, E. L., Bates, T. S., Fehsenfeld, F. C., Goldan, P. D.,  
10 Holloway, J. S., Kuster, W. C., Lerner, B. M., Matthew, B. M., Middlebrook, A. M.,  
11 Onasch, T. B., Peltier, R. E., Quinn, P. K., Senff, C. J., Stohl, A., Sullivan, A. P., Trainer,  
12 M., Warneke, C., Weber, R. J., and Williams, E. J.: Sources of particulate matter in the  
13 northeastern United States in summer: 1. Direct emissions and secondary formation of  
14 organic matter in urban plumes, *J. Geophys. Res.-Atmos.*, 113, D08301,  
15 <https://doi.10.1029/2007jd009243>, 2008.

16 Dette, H. P., Qi, M. A., Schroder, D. C., Godt, A., and Koop, T.: Glass-forming properties of 3-  
17 methylbutane-1,2,3-tricarboxylic acid and its mixtures with water and pinonic acid, *J. Phys.*  
18 *Chem. A*, 118, 7024-7033, 10.1021/jp505910w, 2014.

19 DeRieux, W. S., Li, Y., Lin, P., Laskin, J., Laskin, A., Bertram, A. K., Nizkorodov, S. A., and  
20 Shiraiwa, M.: Predicting the glass transition temperature and viscosity of secondary  
21 organic material using molecular composition, *Atmos. Chem. Phys.*, 18, 6331-6351,  
22 10.5194/acp-18-6331-2018, 2018.

23 Ervens, B., Turpin, B. J., and Weber, R. J.: Secondary organic aerosol formation in cloud  
24 droplets and aqueous particles (aqSOA): a review of laboratory, field and model studies,  
25 *Atmos. Chem. Phys.*, 11, 11069-11102, DOI 10.5194/acp-11-11069-2011, 2011.

26 Evoy, E., Maclean, A. M., Rovelli, G., Li, Y., Tsimpidi, A. P., Karydis, V. A., Kamal, S.,  
27 Lelieveld, J., Shiraiwa, M., Reid, J. P., and Bertram, A. K.: Predictions of diffusion rates  
28 of organic molecules in secondary organic aerosols using the Stokes-Einstein and  
29 fractional Stokes-Einstein relations, *Atmos. Chem. Phys. Discuss.*,  
30 <https://doi.org/10.5194/acp-2019-191>, in review, 2019.

31 Fard, M. M., Krieger, U. K., and Peter, T.: Shortwave radiative impact of liquid-liquid phase  
32 separation in brown carbon aerosols, *Atmos. Chem. Phys.*, 18, 13511-13530, 10.5194/acp-

1 18-13511-2018, 2018.

2 Freedman, M. A.: Phase separation in organic aerosol, *Chem. Soc. Rev.*, 46, 7694-7705,  
3 10.1039/c6cs00783j, 2017.

4 Gentner, D. R., Isaacman, G., Worton, D. R., Chan, A. W. H., Dallmann, T. R., Davis, L., Liu,  
5 S., Day, D. A., Russell, L. M., Wilson, K. R., Weber, R., Guha, A., Harley, R. A., and  
6 Goldstein, A. H.: Elucidating secondary organic aerosol from diesel and gasoline vehicles  
7 through detailed characterization of organic carbon emissions, *Proc. Natl. Acad. Sci. US*,  
8 109, 18318-18323, 10.1073/pnas.1212272109, 2012.

9 Gentner, D. R., Jathar, S. H., Gordon, T. D., Bahreini, R., Day, D. A., El Haddad, I., Hayes, P.  
10 L., Pieber, S. M., Platt, S. M., de Gouw, J., Goldstein, A. H., Harley, R. A., Jimenez, J. L.,  
11 Prevot, A. S. H., and Robinson, A. L.: Review of Urban Secondary Organic Aerosol  
12 Formation from Gasoline and Diesel Motor Vehicle Emissions, *Environ Sci Technol*, 51,  
13 1074-1093, 2017.

14 Gorkowski, K., Beydoun, H., Aboff, M., Walker, J. S., Reid, J. P., and Sullivan, R. C.:  
15 Advanced aerosol optical tweezers chamber design to facilitate phase-separation and  
16 equilibration timescale experiments on complex droplets, *Aerosol. Sci. Tech.*, 50, 1327–  
17 1341, <https://doi.org/10.1080/02786826.2016.1224317>, 2016.

18 Gorkowski, K., Donahue, N. M., and Sullivan, R. C.: Emulsified and Liquid Liquid Phase-  
19 Separated States of alphaPinene Secondary Organic Aerosol Determined Using Aerosol  
20 Optical Tweezers, *Environ. Sci. Technol.*, 51, 12154–12163,  
21 <https://doi.org/10.1021/acs.est.7b03250>, 2017.

22 [Gorkowski, K., Preston, T. C., and Zuend, A.: RH-dependent organic aerosol thermodynamics  
23 via an efficient reduced-complexity model, \*Atmos. Chem. Phys. Discuss.\*,  
24 <https://doi.org/10.5194/acp-2019-495>, in review, 2019.](#)

25 Grayson, J. W., Song, M., Sellier, M., and Bertram, A. K.: Validation of the poke-flow  
26 technique combined with simulations of fluid flow for determining viscosities in samples  
27 with small volumes and high viscosities, *Atmos. Meas. Tech.*, 8, 2463-2472, 2015.

28 Grayson, J. W., Zhang, Y., Mutzel, A., Renbaum-Wolff, L., Boge, O., Kamal, S., Herrmann, H.,  
29 Martin, S. T., and Bertram, A. K.: Effect of varying experimental conditions on the  
30 viscosity of alpha-pinene derived secondary organic material, *Atmos. Chem. Phys.*, 16,  
31 6027-6040, 10.5194/acp-16-6027-2016, 2016.

32 Grayson, J. W., Evoy, E., Song, M., Chu, Y. X., Maclean, A., Nguyen, A., Upshur, M. A.,

1 Ebrahimi, M., Chan, C. K., Geiger, F. M., Thomson, R. J., and Bertram, A. K.: The effect  
2 of hydroxyl functional groups and molar mass on the viscosity of non-crystalline organic  
3 and organic-water particles, *Atmos. Chem. Phys.*, 17, 8509-8524, 10.5194/acp-17-8509-  
4 2017, 2017.

5 Hallquist, M., Wenger, J. C., Baltensperger, U., Rudich, Y., Simpson, D., Claeys, M., Dommen,  
6 J., Donahue, N. M., George, C., Goldstein, A. H., Hamilton, J. F., Herrmann, H., Hoffmann,  
7 T., Iinuma, Y., Jang, M., Jenkin, M. E., Jimenez, J. L., Kiendler-Scharr, A., Maenhaut, W.,  
8 McFiggans, G., Mentel, T. F., Monod, A., Prevot, A. S. H., Seinfeld, J. H., Surratt, J. D.,  
9 Szmigielski, R., and Wildt, J.: The formation, properties and impact of secondary organic  
10 aerosol: current and emerging issues, *Atmos. Chem. Phys.*, 9, 5155-5236, 2009.

11 Ham, S., Babar, Z. B., Lee, J. B., Lim, H.-J., and Song, M.: Liquid–liquid phase separation in  
12 secondary organic aerosol particles produced from  $\alpha$ -pinene ozonolysis and  $\alpha$ -pinene  
13 photooxidation with/without ammonia, *Atmos. Chem. Phys.*, 19, 9321-9331,  
14 <https://doi.org/10.5194/acp-19-9321-2019>, 2019.

15 Hayes, P. L., Carlton, A. G., Baker, K. R., Ahmadov, R., Washenfelder, R. A., Alvarez, S.,  
16 Rappengluck, B., Gilman, J. B., Kuster, W. C., de Gouw, J. A., Zotter, P., Prevot, A. S. H.,  
17 Szidat, S., Kleindienst, T. E., Offenberg, J. H., Ma, P. K., and Jimenez, J. L.: Modeling the  
18 formation and aging of secondary organic aerosols in Los Angeles during CalNex 2010,  
19 *Atmos. Chem. Phys.*, 15, 5773-5801, 10.5194/acp-15-5773-2015, 2015.

20 Hodas, N., Zuend, A., Schilling, K., Berkemeier, T., Shiraiwa, M., Flagan, R. C., and Seinfeld,  
21 J. H.: Discontinuities in hygroscopic growth below and above water saturation for  
22 laboratory surrogates of oligomers in organic atmospheric aerosols, *Atmos. Chem. Phys.*,  
23 16, 12767-12792, 10.5194/acp-16-12767-2016, 2016.

24 Houle, F. A., Hinsberg, W. D., and Wilson, K. R.: Oxidation of a model alkane aerosol by OH  
25 radical: the emergent nature of reactive uptake, *Phys. Chem. Chem. Phys.*, 17, 4412-4423,  
26 2015.

27 IPCC: Climate Change 2013: The Physical science basis. Contribution of working group I to  
28 the fifth assessment report of the intergovernmental panel on climate change, edited by:  
29 Stocker, T. F., Qin, D., Plattner, G.-K., Tignor, M., Allen, S. K., Boschung, J., Nauels, A.,  
30 Xia, Y., Bex, V., and Midgley, P. M., Cambridge University Press, Cambridge, UK and  
31 New York, NY, US, 1535, 2013.

32 Jain, S., Fischer, K. B., and Petrucci, G. A.: The Influence of absolute mass loading of

1 secondary organic aerosols on their phase state, *Atmosphere-Basel*, 9, ARTN 131  
2 10.3390/atmos9040131, 2018.

3 Jang, M., Ghio, A. J., and Cao, G.: Exposure of BEAS-2B cells to secondary organic aerosol  
4 coated on magnetic nanoparticles, *Chem. Res. Toxicol.*, 19, 1044-1050, 2006.

5 Jasper, J. J.: The surface tension of pure liquid compounds, *J. Phys. Chem. Ref. Data*, 1, 841–  
6 1009, <https://doi.org/10.1063/1.3253106>, 1972.

7 Jathar, S. H., Miracolo, M. A., Tkacik, D. S., Donahue, N. M., Adams, P. J., and Robinson, A.  
8 L.: Secondary organic aerosol formation from photo-oxidation of unburned fuel:  
9 Experimental results and implications for aerosol formation from combustion emissions,  
10 *Environ. Sci. Technol.*, 47, 12886-12893, 2013.

11 Jathar, S. H., Donahue, N. M., Adams, P. J., and Robinson, A. L.: Testing secondary organic  
12 aerosol models using smog chamber data for complex precursor mixtures: influence of  
13 precursor volatility and molecular structure, *Atmos. Chem. Phys.*, 14, 5771-5780, 2014.

14 Jathar, S. H., Heppding, C., Link, M. F., Farmer, D. K., Akherati, A., Kleeman, M. J., de Gouw,  
15 J. A., Veres, P. R., and Roberts, J. M.: Investigating diesel engines as an atmospheric source  
16 of isocyanic acid in urban areas, *Atmos. Chem. Phys.*, 17, 8959-8970, 2017.

17 Ji, Z. R., Zhang, Y., Pang, S. F., and Zhang, Y. H.: Crystal nucleation and crystal growth and  
18 mass transfer in internally mixed sucrose/NaNO<sub>3</sub> particles, *J. Phys. Chem. A*, 121, 7968-  
19 7975, [10.1021/acs.jpca.7b08004](https://doi.org/10.1021/acs.jpca.7b08004), 2017.

20 Jimenez, J. L., Canagaratna, M. R., Donahue, N. M., Prevot, A. S. H., Zhang, Q., Kroll, J. H.,  
21 DeCarlo, P. F., Allan, J. D., Coe, H., Ng, N. L., Aiken, A. C., Docherty, K. S., Ulbrich, I.  
22 M., Grieshop, A. P., Robinson, A. L., Duplissy, J., Smith, J. D., Wilson, K. R., Lanz, V. A.,  
23 Hueglin, C., Sun, Y. L., Tian, J., Laaksonen, A., Raatikainen, T., Rautiainen, J., Vaattovaara,  
24 P., Ehn, M., Kulmala, M., Tomlinson, J. M., Collins, D. R., Cubison, M. J., Dunlea, E. J.,  
25 Huffman, J. A., Onasch, T. B., Alfarra, M. R., Williams, P. I., Bower, K., Kondo, Y.,  
26 Schneider, J., Drewnick, F., Borrmann, S., Weimer, S., Demerjian, K., Salcedo, D., Cottrell,  
27 L., Griffin, R., Takami, A., Miyoshi, T., Hatakeyama, S., Shimono, A., Sun, J. Y., Zhang,  
28 Y. M., Dzepina, K., Kimmel, J. R., Sueper, D., Jayne, J. T., Herndon, S. C., Trimborn, A.  
29 M., Williams, L. R., Wood, E. C., Middlebrook, A. M., Kolb, C. E., Baltensperger, U., and  
30 Worsnop, D. R.: Evolution of organic aerosols in the atmosphere, *Science*, 326, 1525-1529,  
31 <https://doi.org/10.1126/science.1180353>, 2009.

32 Kanakidou, M., Seinfeld, J. H., Pandis, S. N., Barnes, I., Dentener, F. J., Facchini, M. C., Van

1 Dingenen, R., Ervens, B., Nenes, A., Nielsen, C. J., Swietlicki, E., Putaud, J. P., Balkanski,  
2 Y., Fuzzi, S., Horth, J., Moortgat, G. K., Winterhalter, R., Myhre, C. E. L., Tsigaridis, K.,  
3 Vignati, E., Stephanou, E. G., and Wilson, J.: Organic aerosol and global climate  
4 modelling: a review, *Atmos. Chem. Phys.*, 5, 1053-1123, 2005.

5 Kidd, C., Perraud, V., Wingen, L. M., and Finlayson-Pitts, B. J.: Integrating phase and  
6 composition of secondary organic aerosol from the ozonolysis of alpha-pinene, *P. Natl.*  
7 *Acad. Sci. USA*, 111, 7552-7557, <https://doi.org/10.1073/pnas.1322558111>, 2014.

8 Kim, Y., Sartelet, K., and Couvidat, F.: Modeling the effect of non-ideality, dynamic mass  
9 transfer and viscosity on SOA formation in a 3-D air quality model, *Atmos. Chem. Phys.*,  
10 19, 1241-1261, [10.5194/acp-19-1241-2019](https://doi.org/10.5194/acp-19-1241-2019), 2019.

11 Knopf, D. A.: Thermodynamic properties and nucleation processes of upper tropospheric and  
12 lower stratospheric aerosol particles, Diss. ETH No. 15103, Zurich, Switzerland, 2003.

13 Knopf, D. A., Alpert, P. A., and Wang, B. B.: The Role of Organic Aerosol in Atmospheric Ice  
14 Nucleation: A Review, *Acs. Earth Space Chem.*, 2, 168-202,  
15 [10.1021/acsearthspacechem.7b00120](https://doi.org/10.1021/acsearthspacechem.7b00120), 2018.

16 Koop, T., Bookhold, J., Shiraiwa, M., and Poschl, U.: Glass transition and phase state of organic  
17 compounds: dependency on molecular properties and implications for secondary organic  
18 aerosols in the atmosphere, *Phys. Chem. Chem. Phys.*, 13, 19238-19255,  
19 <https://doi.org/10.1039/C1cp22617g>, 2011.

20 Krieger, U. K., Marcolli, C., and Reid, J. P.: Exploring the complexity of aerosol particle  
21 properties and processes using single particle techniques, *Chem. Soc. Rev.*, 41, 6631-6662,  
22 <https://doi.org/10.1039/c2cs35082c>, 2012.

23 Kuwata, M., and Martin, S. T.: Phase of atmospheric secondary organic material affects its  
24 reactivity, *P. Natl. Acad. Sci. USA*, 109, 17354-17359, 2012.

25 Kwamena, N. O. A., Buajarern, J., and Reid, J. P.: Equilibrium Morphology of Mixed  
26 Organic/Inorganic/Aqueous Aerosol Droplets: Investigating the effect of RH and  
27 surfactants, *J. Phys. Chem. A*, 114, 5787-5795, <https://doi.org/10.1021/Jp1003648>, 2010.

28 Ladino, L. A., Zhou, S., Yakobi-Hancock, J. D., Aljawhary, D., and Abbatt, J. P. D.: Factors  
29 controlling the ice nucleating abilities of alpha-pinene SOA particles, *J. Geophys. Res.-*  
30 *Atmos.*, 119, 9041-9051, 2014.

31 Lambe, A. T., Onasch, T. B., Massoli, P., Croasdale, D. R., Wright, J. P., Ahern, A. T.,  
32 Williams, L. R., Worsnop, D. R., Brune, W. H., and Davidovits, P.: Laboratory studies of

1 the chemical composition and cloud condensation nuclei (CCN) activity of secondary  
2 organic aerosol (SOA) and oxidized primary organic aerosol (OPOA), *Atmos. Chem.*  
3 *Phys.*, 11, 8913-8928, DOI 10.5194/acp-11-8913-2011, 2011.

4 Li, Y. J., Liu, P., Gong, Z., Wang, Y., Bateman, A. P., Bergoend, C., Bertram, A. K., and Martin,  
5 S. T.: Chemical reactivity and liquid/nonliquid states of secondary organic material,  
6 *Environ. Sci. and Tech.*, 49, 13264-13274, 10.1021/acs.est.5b03392, 2015.

7 Li, Z. Y., Smith, K. A., and Cappa, C. D.: Influence of relative humidity on the heterogeneous  
8 oxidation of secondary organic aerosol, *Atmos. Chem. Phys.*, 18, 14585-14608,  
9 10.5194/acp-18-14585-2018, 2018.

10 Liu, S., Ahlm, L., Day, D. A., Russell, L. M., Zhao, Y. L., Gentner, D. R., Weber, R. J.,  
11 Goldstein, A. H., Jaoui, M., Offenberg, J. H., Kleindienst, T. E., Rubitschun, C., Surratt, J.  
12 D., Sheesley, R. J., and Scheller, S.: Secondary organic aerosol formation from fossil fuel  
13 sources contribute majority of summertime organic mass at Bakersfield, *J. Geophys. Res-*  
14 *Atmos.*, 117, 2012.

15 Liu, P. F., Li, Y. J., Wang, Y., Gilles, M. K., Zaveri, R. A., Bertram, A. K., and Martin, S. T.:  
16 Lability of secondary organic particulate matter, *P. Natl. Acad. Sci. US*, 113, 12643-12648,  
17 10.1073/pnas.1603138113, 2016.

18 Liu, P., Song, M., Zhao, T., Gunthe, S. S., Ham, S., He, Y., Qin, Y. M., Gong, Z., Amorim, J.  
19 C., Bertram, A. K., and Martin, S. T.: Resolving the mechanisms of hygroscopic growth  
20 and cloud condensation nuclei activity for organic particulate matter, *Nat. Commun.*, 9,  
21 4076, 10.1038/s41467-018-06622-2, 2018.

22 Loza, C. L., Coggon, M. M., Nguyen, T. B., Zuend, A., Flagan, R. C., and Seinfeld, J. H.: On  
23 the mixing and evaporation of secondary organic aerosol components, *Environ. Sci.*  
24 *Technol.*, 47, 6173-6180, 10.1021/es400979k, 2013.

25 Maclean, A. M., Butenhoff, C. L., Grayson, J. W., Barsanti, K., Jimenez, J. L., and Bertram, A.  
26 K.: Mixing times of organic molecules within secondary organic aerosol particles: a global  
27 planetary boundary layer perspective, *Atmos. Chem. Phys.*, 17, 13037-13048,  
28 10.5194/acp-17-13037-2017, 2017.

29 Marcolli, C., Luo, B., Peter, T.: Mixing of the organic aerosol fractions: Liquids as the  
30 thermodynamically stable phases, *J. Phys. Chem. A*, 108, 2216-2224, 10.1021/jp036080l,  
31 2004.

32 Marcolli, C. and Krieger, U. K.: Phase changes during hygroscopic cycles of mixed

1 organic/inorganic model systems of tropospheric aerosols, *J. Phys. Chem. A*, 110, 1881–  
2 1893, <https://doi.org/10.1021/Jp0556759>, 2006.

3 Marshall, F. H., Miles, R. E. H., Song, Y. C., Ohm, P. B., Power, R. M., Reid, J. P., and Dutcher,  
4 C. S.: Diffusion and reactivity in ultraviscous aerosol and the correlation with particle  
5 viscosity, *Chem. Sci.*, 7, 1298-1308, [10.1039/c5sc03223g](https://doi.org/10.1039/c5sc03223g), 2016.

6 Martin, S. T., Andreae, M. O., Althausen, D., Artaxo, P., Baars, H., Borrmann, S., Chen, Q.,  
7 Farmer, D. K., Guenther, A., Gunthe, S. S., Jimenez, J. L., Karl, T., Longo, K., Manzi, A.,  
8 Müller, T., Pauliquevis, T., Petters, M. D., Prenni, A. J., Pöschl, U., Rizzo, L. V., Schneider,  
9 J., Smith, J. N., Swietlicki, E., Tota, J., Wang, J., Wiedensohler, A., and Zorn, S. R.: An  
10 overview of the Amazonian aerosol characterization experiment 2008 (AMAZE-08),  
11 *Atmos. Chem. Phys.*, 10, 11415–11438, <https://doi.org/10.5194/acp-10-11415-2010>, 2010.

12 Massoli, P., Lambe, A. T., Ahern, A. T., Williams, L. R., Ehn, M., Mikkila, J., Canagaratna, M.  
13 R., Brune, W. H., Onasch, T. B., Jayne, J. T., Petaja, T., Kulmala, M., Laaksonen, A., Kolb,  
14 C. E., Davidovits, P., and Worsnop, D. R.: Relationship between aerosol oxidation level  
15 and hygroscopic properties of laboratory generated secondary organic aerosol (SOA)  
16 particles, *Geophys. Res. Lett.*, 37, Artn L24801, [10.1029/2010gl045258](https://doi.org/10.1029/2010gl045258), 2010.

17 Mu, Q., Shiraiwa, M., Octaviani, M., Ma, N., Ding, A. J., Su, H., Lammel, G., Poschl, U., and  
18 Cheng, Y. F.: Temperature effect on phase state and reactivity controls atmospheric  
19 multiphase chemistry and transport of PAHs, *Sci. Adv.*, 4, UNSP eaap7314  
20 [10.1126/sciadv.aap7314](https://doi.org/10.1126/sciadv.aap7314), 2018.

21 Murray, B. J.: Inhibition of ice crystallisation in highly viscous aqueous organic acid droplets,  
22 *Atmos. Chem. Phys.*, 8, 5423-5433, 2008.

23 Murray, B. J., and Bertram, A. K.: Inhibition of solute crystallisation in aqueous  $\text{H}^+\text{-NH}_4^+$ -  
24  $\text{SO}_4^{2-}\text{-H}_2\text{O}$  droplets, *Phys. Chem. Chem. Phys.*, 10, 3287-3301, 2008.

25 Murray, B. J., Wilson, T. W., Dobbie, S., Cui, Z. Q., Al-Jumur, S. M. R. K., Mohler, O.,  
26 Schnaiter, M., Wagner, R., Benz, S., Niemand, M., Saathoff, H., Ebert, V., Wagner, S., and  
27 Karcher, B.: Heterogeneous nucleation of ice particles on glassy aerosols under cirrus  
28 conditions, *Nat. Geosci.*, 3, 233-237, <https://doi.org/10.1038/Ngeo817>, 2010.

29 Murray, B. J., Haddrell, A. E., Peppe, S., Davies, J. F., Reid, J. P., O'Sullivan, D., Price, H. C.,  
30 Kumar, R., Saunders, R. W., Plane, J. M. C., Umo, N. S., and Wilson, T. W.: Glass  
31 formation and unusual hygroscopic growth of iodic acid solution droplets with relevance  
32 for iodine mediated particle formation in the marine boundary layer, *Atmos. Chem. Phys.*,

1 12, 8575-8587, <https://doi.org/10.5194/acp-12-8575-2012>, 2012.

2 O'Brien, R. E., Wang, B. B., Kelly, S. T., Lundt, N., You, Y., Bertram, A. K., Leone, S. R.,  
3 Laskin, A., and Gilles, M. K.: Liquid-Liquid Phase Separation in Aerosol Particles:  
4 Imaging at the Nanometer Scale, *Environ. Sci. Technol.*, 49, 4995–5002,  
5 <https://doi.org/10.1021/acs.est.5b00062>, 2015.

6 Odum, J. R., Jungkamp, T. P. W., Griffin, R. J., Flagan, R. C., and Seinfeld, J. H.: The  
7 atmospheric aerosol-forming potential of whole gasoline vapor, *Science*, 276, 96-99,  
8 <https://doi.org/10.1126/science.276.5309.96>, 1997.

9 Ovadnevaite, J., Zuend, A., Laaksonen, A., Sanchez, K. J., Roberts, G., Ceburnis, D., Decesari,  
10 S., Rinaldi, M., Hodas, N., Facchini, M. C., Seinfeld, J. H., and Dowd, C. O.: Surface  
11 tension prevails over solute effect in organic-influenced cloud droplet activation, *Nature*,  
12 546, 637-641, [10.1038/nature22806](https://doi.org/10.1038/nature22806), 2017.

13 Pajunoja, A., Malila, J., Hao, L. Q., Joutsensaari, J., Lehtinen, K. E. J., and Virtanen, A.:  
14 Estimating the viscosity range of SOA particles based on their coalescence time, *Aerosol*  
15 *Sci. Tech.*, 48, I-Iv, <https://doi.org/10.1080/02786826.2013.870325>, 2014.

16 Pandis, S. N., Harley, R. A., Cass, G. R., and Seinfeld, J. H.: Secondary organic aerosol  
17 formation and transport, *Atmos. Environ. A-Gen.*, 26, 2269–2282, 1992.

18 Pankow, J. F.: Gas/particle partitioning of neutral and ionizing compounds to single and multi-  
19 phase aerosol particles. 1. Unified modeling framework, *Atmos. Environ.*, 37, 3323–3333,  
20 [https://doi.org/10.1016/S1352-2310\(03\)00346-7](https://doi.org/10.1016/S1352-2310(03)00346-7), 2003.

21 Pant, A., Parsons, M. T., and Bertram, A. K.: Crystallization of aqueous ammonium sulfate  
22 particles internally mixed with soot and kaolinite: Crystallization relative humidities and  
23 nucleation rates, *J. Phys. Chem. A*, 110, 8701-8709, <https://doi.org/10.1021/Jp060985s>, 2006.

24 Parsons, M. T., Mak, J., Lipetz, S. R., and Bertram, A. K.: Deliquescence of malonic, succinic,  
25 glutaric, and adipic acid particles, *J. Geophys. Res.-Atmos.*, 109, D06212,  
26 <https://doi.org/10.1029/2003jd004075>, 2004.

27 Perraud, V., Bruns, E. A., Ezell, M. J., Johnson, S. N., Yu, Y., Alexander, M. L., Zelenyuk, A.,  
28 Imre, D., Chang, W. L., Dabdub, D., Pankow, J. F., and Finlayson-Pitts, B. J.:  
29 Nonequilibrium atmospheric secondary organic aerosol formation and growth, *P. Natl.*  
30 *Acad. Sci. USA*, 109, 2836-2841, <https://doi.org/10.1073/pnas.1119909109>, 2012.

31 Petters, M. D., and Kreidenweis, S. M.: A single parameter representation of hygroscopic  
32 growth and cloud condensation nucleus activity, *Atmos. Chem. Phys.*, 7, 1961-1971,



1 <https://doi.10.5194/acp-7-1961-2007>, 2007.

2 Petters, M. D., Kreidenweis, S. M., Snider, J. R., Koehler, K. A., Wang, Q., Prenni, A. J., and  
3 Demott, P. J.: Cloud droplet activation of polymerized organic aerosol, *Tellus B*, 58, 196-  
4 205, DOI 10.1111/j.1600-0889.2006.00181.x, 2006.

5 Pöschl, U., Martin, S. T., Sinha, B., Chen, Q., Gunthe, S. S., Huffman, J. A., Borrmann, S.,  
6 Farmer, D. K., Garland, R. M., Helas, G., Jimenez, J. L., King, S. M., Manzi, A., Mikhailov,  
7 E., Pauliquevis, T., Petters, M. D., Prenni, A. J., Roldin, P., Rose, D., Schneider, J., Su, H.,  
8 Zorn, S. R., Artaxo, P., and Andreae, M. O.: Rainforest aerosols as biogenic nuclei of  
9 clouds and precipitation in the Amazon., *Science*, 329, 1513–1516,  
10 <https://doi.org/10.1126/science.1191056>, 2010.

11 Pöschl, U., and Shiraiwa, M.: Multiphase Chemistry at the Atmosphere-Biosphere Interface  
12 Influencing Climate and Public Health in the Anthropocene, *Chem. Rev.*, 115, 4440-4475,  
13 <https://doi.10.1021/cr500487s>, 2015.

14 Price, H. C., Mattsson, J., and Murray, B. J.: Sucrose diffusion in aqueous solution, *Phys. Chem.*  
15 *Chem. Phys.*, 18, 19207-19216, <https://doi.10.1039/c6cp03238a>, 2016.

16 Price, H. C., Mattsson, J., Zhang, Y., Bertram, A. K., Davies, J. F., Grayson, J. W., Martin, S.  
17 T., O'Sullivan, D., Reid, J. P., Rickards, A. M. J., and Murray, B. J.: Water diffusion in  
18 atmospherically relevant alpha-pinene secondary organic material, *Chem. Sci.*, 6, 4876-  
19 4883, 10.1039/c5sc00685f, 2015.

20 Pye, H. O. T., Chan, A. W. H., Barkley, M. P., and Seinfeld, J. H.: Global modeling of organic  
21 aerosol: the importance of reactive nitrogen (NO<sub>x</sub> and NO<sub>3</sub>), *Atmos. Chem. Phys.*, 10,  
22 11261-11276, 10.5194/acp-10-11261-2010, 2010.

23 Rastak, N., Pajunoja, A., Navarro, J. C. A., Ma, J., Song, M., Partridge, D. G., Kirkevåg, A.,  
24 Leong, Y., Hu, W. W., Taylor, N. F., Lambe, A., Cerully, K., Bougiatioti, A., Liu, P., Krejci,  
25 R., Petaja, T., Percival, C., Davidovits, P., Worsnop, D. R., Ekman, A. M. L., Nenes, A.,  
26 Martin, S., Jimenez, J. L., Collins, D. R., Topping, D. O., Bertram, A. K., Zuend, A.,  
27 Virtanen, A., and Riipinen, I.: Microphysical explanation of the RH-dependent water  
28 affinity of biogenic organic aerosol and its importance for climate, *Geophys. Res. Lett.*,  
29 44, 5167–5177, <https://doi.org/10.1002/2017gl073056>, 2017.

30 Riipinen, I., Pierce, J. R., Yli-Juuti, T., Nieminen, T., Hakkinen, S., Ehn, M., Junninen, H.,  
31 Lehtipalo, K., Petaja, T., Slowik, J., Chang, R., Shantz, N. C., Abbatt, J., Leaitch, W. R.,  
32 Kerminen, V. M., Worsnop, D. R., Pandis, S. N., Donahue, N. M., and Kulmala, M.:

1 Organic condensation: a vital link connecting aerosol formation to cloud condensation  
2 nuclei (CCN) concentrations, *Atmos. Chem. Phys.*, 11, 3865-3878, DOI 10.5194/acp-11-  
3 3865-2011, 2011.

4 Reid, J. P., Bertram, A. K., Topping, D. O., Laskin, A., Martin, S. T., Petters, M. D., Pope, F.  
5 D., and Rovelli, G.: The viscosity of atmospherically relevant organic particles, *Nat.*  
6 *Commun.*, 9, ARTN 956 10.1038/s41467-018-03027-z, 2018.

7 Reid, J. P., Dennis-Smith, B. J., Kwamena, N. O. A., Miles, R. E. H., Hanford, K. L., and  
8 Homer, C. J.: The morphology of aerosol particles consisting of hydrophobic and  
9 hydrophilic phases: hydrocarbons, alcohols and fatty acids as the hydrophobic component,  
10 *Phys. Chem. Chem. Phys.*, 13, 15559–15572, <https://doi.org/10.1039/C1cp21510h>, 2011.

11 Reist, P.: *Aerosol science and technology*, McGraw-Hill Professional, New York, NY, USA, 2  
12 Edn., 1992.

13 Renbaum-Wolff, L., Grayson, J. W., Bateman, A. P., Kuwata, M., Sellier, M., Murray, B. J.,  
14 Shilling, J. E., Martin, S. T., and Bertram, A. K.: Viscosity of alpha-pinene secondary  
15 organic material and implications for particle growth and reactivity, *Proc. Natl. Acad. Sci.*  
16 *US*, 110, 8014-8019, <https://doi.org/10.1073/pnas.1219548110>, 2013.

17 Renbaum-Wolff, L., Song, M., Marcolli, C., Zhang, Y., Liu, P. F., Grayson, J. W., Geiger, F. M.,  
18 Martin, S. T., and Bertram, A. K.: Observations and implications of liquid-liquid phase  
19 separation at high relative humidities in secondary organic material produced by  $\alpha$ -pinene  
20 ozonolysis without inorganic salts, *Atmos. Chem. Phys.*, 16, 7969–7979,  
21 <https://doi.org/10.5194/acp16-7969-2016>, 2016.

22 Roach, P. J., Laskin, J., and Laskin, A.: Molecular characterization of organic aerosols using  
23 nanospray-desorption/electrospray ionization-mass spectrometry, *Anal. Chem.*, 82, 7979-  
24 7986, 10.1021/ac101449p, 2010.

25 Robinson, E. S., Saleh, R., and Donahue, N. M.: Organic aerosol mixing observed by single-  
26 particle mass spectrometry, *J. Phys. Chem. A*, 117, 13935-13945,  
27 <https://doi.10.1021/Jp405789t>, 2013.

28 Rothfuss, N. E., and Petters, M. D.: Influence of functional groups on the viscosity of organic  
29 aerosol, *Environ. Sci. Technol.*, 51, 271-279, 10.1021/acs.est.6b04478, 2017.

30 Saukko, E., Lambe, A. T., Massoli, P., Koop, T., Wright, J. P., Croasdale, D. R., Pedernera, D.  
31 A., Onasch, T. B., Laaksonen, A., Davidovits, P., Worsnop, D. R., and Virtanen, A.:  
32 Humidity-dependent phase state of SOA particles from biogenic and anthropogenic

1 precursors, *Atmos. Chem. Phys.*, 12, 7517-7529, <https://doi.10.5194/acp-12-7517-2012>,  
2 2012.

3 Schauer, J. J., Fraser, M. P., Cass, G. R., and Simoneit, B. R. T.: Source reconciliation of  
4 atmospheric gas-phase and particle-phase pollutants during a severe photochemical smog  
5 episode, *Environ. Sci. Technol.*, 36, 3806-3814, <https://doi.10.1021/Es011458j>, 2002a.

6 Schauer, J. J., Kleeman, M. J., Cass, G. R., and Simoneit, B. R. T.: Measurement of emissions  
7 from air pollution sources. 5. C-1-C-32 organic compounds from gasoline-powered motor  
8 vehicles, *Environ. Sci. Technol.*, 36, 1169-1180, <https://doi.10.1021/Es0108077>, 2002b.

9 Schill, G. P., De Haan, D. O., and Tolbert, M. A.: Heterogeneous ice nucleation on simulated  
10 secondary organic aerosol, *Environ. Sci. Technol.*, 48, 1675-1682, 2014.

11 Seinfeld, J. H., and Pandis, S. N.: *Atmospheric chemistry and physics*, A Wiley-interscience  
12 publication, 2006.

13 Shiraiwa, M., Ammann, M., Koop, T., and Poschl, U.: Gas uptake and chemical aging of  
14 semisolid organic aerosol particles, *Proc. Natl. Acad. Sci. US*, 108, 11003-11008,  
15 <https://doi.10.1073/pnas.1103045108>, 2011.

16 Shiraiwa, M., and Seinfeld, J. H.: Equilibration timescale of atmospheric secondary organic  
17 aerosol partitioning, *Geophys. Res. Lett.*, 39, L24801, <https://doi.10.1029/2012gl054008>,  
18 2012.

19 Shiraiwa, M., Yee, L. D., Schilling, K. A., Loza, C. L., Craven, J. S., Zuend, A., Ziemann, P. J.,  
20 and Seinfeld, J. H.: Size distribution dynamics reveal particle-phase chemistry in organic  
21 aerosol formation, *Proc. Natl. Acad. Sci. USA*, 110, 11746-11750,  
22 <https://doi.10.1073/pnas.1307501110>, 2013.

23 Shiraiwa, M., Zuend, A., Bertram, A. K., and Seinfeld, J. H.: Gas particle partitioning of  
24 atmospheric aerosols: interplay of physical state, non-ideal mixing and morphology, *Phys.*  
25 *Chem. Chem. Phys.*, 15, 11441-11453, <https://doi.org/10.1039/C3cp51595h>, 2013.

26 Shiraiwa, M., Li, Y., Tsimpidi, A. P., Karydis, V. A., Berkemeier, T., Pandis, S. N., Lelieveld,  
27 J., Koop, T., and Poschl, U.: Global distribution of particle phase state in atmospheric  
28 secondary organic aerosols, *Nat. Commun.*, 8, 15002, <https://doi.10.1038/ncomms15002>,  
29 2017.

30 Shrivastava, M., Cappa, C. D., Fan, J. W., Goldstein, A. H., Guenther, A. B., Jimenez, J. L.,  
31 Kuang, C., Laskin, A., Martin, S. T., Ng, N. L., Petaja, T., Pierce, J. R., Rasch, P. J., Roldin,  
32 P., Seinfeld, J. H., Shilling, J., Smith, J. N., Thornton, J. A., Volkamer, R., Wang, J.,

1 Worsnop, D. R., Zaveri, R. A., Zelenyuk, A., and Zhang, Q.: Recent advances in  
2 understanding secondary organic aerosol: Implications for global climate forcing, *Rev.*  
3 *Geophys.*, 55, 509-559, 10.1002/2016rg000540, 2017.

4 Shrivastava, M., Lou, S., Zelenyuk, A., Easter, R. C., Corley, R. A., Thrall, B. D., Rasch, P. J.,  
5 Fast, J. D., Simonich, S. L. M., Shen, H. Z., and Tao, S.: Global long-range transport and  
6 lung cancer risk from polycyclic aromatic hydrocarbons shielded by coatings of organic  
7 aerosol, *Proc. Natl. Acad. Sci. US*, 114, 1246-1251, 10.1073/pnas.1618475114, 2017.

8 Solomon, S.: *Climate change 2007-the physical science basis: Working group I contribution to*  
9 *the fourth assessment report of the IPCC*, Cambridge University Press, 2007.

10 Song, M., Marcolli, C., Krieger, U. K., Zuend, A., and Peter, T.: LLPS and morphology of  
11 internally mixed dicarboxylic acids/ammonium sulfate/water particles, *Atmos. Chem.*  
12 *Phys.*, 12, 2691-2712, <https://doi.10.5194/acp-12-2691-2012>, 2012a.

13 Song, M., Marcolli, C., Krieger, U. K., Zuend, A., and Peter, T.: Liquid-liquid phase separation  
14 in aerosol particles: Dependence on O: C, organic functionalities, and compositional  
15 complexity, *Geophys. Res. Lett.*, 39, L19801, <https://doi.org/10.1029/2012gl052807>,  
16 2012b.

17 Song, M. J., Marcolli, C., Krieger, U. K., Lienhard, D. M., and Peter, T.: Morphologies of  
18 mixed organic/inorganic/aqueous aerosol droplets, *Faraday Discuss.*, 165, 289-316,  
19 <https://doi.10.1039/C3fd00049d>, 2013.

20 Song, M., Liu, P. F., Hanna, S. J., Li, Y. J., Martin, S. T., and Bertram, A. K.: RH-dependent  
21 viscosities of isoprene-derived secondary organic material and atmospheric implications  
22 for isoprene-dominant forests, *Atmos. Chem. Phys.*, 15, 5145-5159, 2015.

23 Song, M., Liu, P. F. F., Hanna, S. J., Zaveri, R. A., Potter, K., You, Y., Martin, S. T., and Bertram,  
24 A. K.: RH-dependent viscosity of secondary organic material from toluene photo-  
25 oxidation and possible implications for organic particulate matter over megacities, *Atmos.*  
26 *Chem. Phys.*, 16, 8817-8830, 10.5194/acp-16-8817-2016, 2016a.

27 Song, Y. C., Haddrell, A. E., Bzdek, B. R., Reid, J. P., Barman, T., Topping, D. O., Percival, C.,  
28 and Cai, C.: Measurements and predictions of binary component aerosol particle viscosity,  
29 *J. Phys. Chem. A*, 120, 8123-8137, 10.1021/acs.jpca.6b07835, 2016b.

30 Song, M., Liu, P., Martin, S. T., Bertram, A. K.: Liquid-liquid phase separation in particles  
31 containing secondary organic material free of inorganic salts, *Atmos. Chem. Phys.*, 17,  
32 11261-11271, <https://doi.org/10.5194/acp-17-11261-2017>, 2017.

1 Song, M., Ham, S., Andrews, R. J., You, Y., Bertram, A. K.: Liquid–liquid phase separation in  
2 organic particles containing one and two organic species: importance of the average O: C,  
3 Atmos. Chem. Phys., 18, 12075-12084, <https://doi.org/10.5194/acp-18-12075-2018>, 2018.

4 Steimer, S. S., Lampimaki, M., Coz, E., Grzanic, G., and Ammann, M.: The influence of  
5 physical state on shikimic acid ozonolysis: a case for in situ microspectroscopy, Atmos.  
6 Chem. Phys., 14, 10761-10772, 2014.

7 Ullmann, D. A., Hinks, M. L., Maclean, A. M., Butenhoff, C. L., Grayson, J. W., Barsanti, K.,  
8 Jimenez, J. L., Nizkorodov, S. A., Kamal, S., and Bertram, A. K.: Viscosities, diffusion  
9 coefficients, and mixing times of intrinsic fluorescent organic molecules in brown  
10 limonene secondary organic aerosol and tests of the Stokes–Einstein equation, Atmos.  
11 Chem. Phys., 19, 1491-1503, <https://doi.org/10.5194/acp-19-1491-2019>, 2019.

12 Veghte, D. P., Altaf, M. B., and Freedman, M. A.: Size dependence of the structure of organic  
13 aerosol, J. Am. Chem. Soc., 135, 16046–16049, 10.1021/ja408903g, 2013.

14 Velasco, E., Lamb, B., Westberg, H., Allwine, E., Sosa, G., Arriaga-Colina, J. L., Jobson, B. T.,  
15 Alexander, M. L., Prazeller, P., Knighton, W. B., Rogers, T. M., Grutter, M., Herndon, S.  
16 C., Kolb, C. E., Zavala, M., de Foy, B., Volkamer, R., Molina, L. T., and Molina, M. J.:  
17 Distribution, magnitudes, reactivities, ratios and diurnal patterns of volatile organic  
18 compounds in the Valley of Mexico during the MCMA 2002 & 2003 field campaigns,  
19 Atmos. Chem. Phys., 7, 329-353, 2007.

20 Velasco, E., Pressley, S., Grivicke, R., Allwine, E., Coons, T., Foster, W., Jobson, B. T.,  
21 Westberg, H., Ramos, R., Hernandez, F., Molina, L. T., and Lamb, B.: Eddy covariance  
22 flux measurements of pollutant gases in urban Mexico City, Atmos. Chem. Phys., 9, 7325-  
23 7342, 2009.

24 Virtanen, A., Joutsensaari, J., Koop, T., Kannosto, J., Yli-Pirila, P., Leskinen, J., Makela, J. M.,  
25 Holopainen, J. K., Poschl, U., Kulmala, M., Worsnop, D. R., and Laaksonen, A.: An  
26 amorphous solid state of biogenic secondary organic aerosol particles, Nature, 467, 824-  
27 827, 10.1038/nature09455, 2010.

28 Vutukuru, S., Griffin, R. J., and Dabdub, D.: Simulation and analysis of secondary organic  
29 aerosol dynamics in the South Coast Air Basin of California, J. Geophys. Res.-Atmos.,  
30 111, 2006.

31 Wang, B. B., Lambe, A. T., Massoli, P., Onasch, T. B., Davidovits, P., Worsnop, D. R., and  
32 Knopf, D. A.: The deposition ice nucleation and immersion freezing potential of

1 amorphous secondary organic aerosol: Pathways for ice and mixed-phase cloud formation,  
2 J. Geophys. Res.-Atmos., 117, D16209, <https://doi.10.1029/2012jd018063>, 2012.

3 Wang, B. B., O'Brien, R. E., Kelly, S. T., Shilling, J. E., Moffet, R. C., Gilles, M. K., and Laskin,  
4 A.: Reactivity of liquid and semisolid secondary organic carbon with chloride and nitrate  
5 in atmospheric aerosols, J. of Phys. Chem. A, 119, 4498-4508, 2015.

6 Wang, L. N., Cai, C., and Zhang, Y. H.: Kinetically determined hygroscopicity and  
7 efflorescence of sucrose-ammonium sulfate aerosol droplets under lower RH, J. Phys.  
8 Chem. B, 121, 8551-8557, [10.1021/acs.jpcc.7b05551](https://doi.10.1021/acs.jpcc.7b05551), 2017.

9 Wilson, T. W., Murray, B. J., Wagner, R., Mohler, O., Saathoff, H., Schnaiter, M., Skrotzki, J.,  
10 Price, H. C., Malkin, T. L., Dobbie, S., and Al-Jumur, S. M. R. K.: Glassy aerosols with a  
11 range of compositions nucleate ice heterogeneously at cirrus temperatures, Atmos. Chem.  
12 Phys., 12, 8611-8632, 2012.

13 Ye, Q., Robinson, E. S., Ding, X., Ye, P. L., Sullivan, R. C., and Donahue, N. M.: Mixing of  
14 secondary organic aerosols versus relative humidity, Proc. Natl. Acad. Sci. US, 113,  
15 12649-12654, [10.1073/pnas.1604536113](https://doi.10.1073/pnas.1604536113), 2016.

16 Ye, Q., Upshur, M. A., Robinson, E. S., Geiger, F. M., Sullivan, R. C., Thomson, R. J., and  
17 Donahue, N. M.: Following particle-particle mixing in atmospheric secondary organic  
18 aerosols by using isotopically labeled terpenes, Chem.-Us, 4, 318-333,  
19 [10.1016/j.chempr.2017.12.008](https://doi.10.1016/j.chempr.2017.12.008), 2018.

20 Yli-Juuti, T., Pajunoja, A., Tikkanen, O. P., Buchholz, A., Faiola, C., Vaisanen, O., Hao, L. Q.,  
21 Kari, E., Perakyla, O., Garmash, O., Shiraiwa, M., Ehn, M., Lehtinen, K., and Virtanen,  
22 A.: Factors controlling the evaporation of secondary organic aerosol from alpha-pinene  
23 ozonolysis, Geophys. Res. Lett., 44, 2562-2570, [10.1002/2016gl072364](https://doi.10.1002/2016gl072364), 2017.

24 You, Y., Smith, M. L., Song, M. J., Martin, S. T., and Bertram, A. K.: Liquid-liquid phase  
25 separation in atmospherically relevant particles consisting of organic species and inorganic  
26 salts, Int. Rev. Phys. Chem., 33, 43-77, <https://doi.org/10.1080/0144235X.2014.890786>,  
27 2014.

28 Zaveri, R. A., Easter, R. C., Shilling, J. E., and Seinfeld, J. H.: Modeling kinetic partitioning of  
29 secondary organic aerosol and size distribution dynamics: representing effects of volatility,  
30 phase state, and particle-phase reaction, Atmos. Chem. Phys., 14, 5153-5181,  
31 <https://doi.10.5194/acp-14-5153-2014>, 2014.

32 Zaveri, R. A., Shilling, J. E., Zelenyuk, A., Liu, J. M., Bell, D. M., D'Ambro, E. L., Gaston, C.,

1 Thornton, J. A., Laskin, A., Lin, P., Wilson, J., Easter, R. C., Wang, J., Bertram, A. K.,  
2 Martin, S. T., Seinfeld, J. H., and Worsnop, D. R.: Growth kinetics and size distribution  
3 dynamics of viscous secondary organic aerosol, *Environ. Sci. Technol.*, 52, 1191-1199,  
4 10.1021/acs.est.7b04623, 2018.

5 Zelenyuk, A., Imre, D., Beranek, J., Abramson, E., Wilson, J., and Shrivastava, M.: Synergy  
6 between secondary organic aerosols and long-range transport of polycyclic aromatic  
7 hydrocarbons, *Environ. Sci. Technol.*, 46, 12459-12466, <https://doi.10.1021/Es302743z>,  
8 2012.

9 Zhang, Q., Jimenez, J. L., Canagaratna, M. R., Allan, J. D., Coe, H., Ulbrich, I., Alfarra, M. R.,  
10 Takami, A., Middlebrook, A. M., Sun, Y. L., Dzepina, K., Dunlea, E., Docherty, K.,  
11 DeCarlo, P. F., Salcedo, D., Onasch, T., Jayne, J. T., Miyoshi, T., Shimonono, A., Hatakeyama,  
12 S., Takegawa, N., Kondo, Y., Schneider, J., Drewnick, F., Borrmann, S., Weimer, S.,  
13 Demerjian, K., Williams, P., Bower, K., Bahreini, R., Cottrell, L., Griffin, R. J., Rautiainen,  
14 J., Sun, J. Y., Zhang, Y. M., and Worsnop, D. R.: Ubiquity and dominance of oxygenated  
15 species in organic aerosols in anthropogenically-influenced Northern Hemisphere  
16 midlatitudes, *Geophys. Res. Lett.*, 34, L13801, <https://doi.10.1029/2007gl029979>, 2007.

17 Zhang, Y., Chen, Y. Z., Lambe, A. T., Olson, N. E., Lei, Z. Y., Craig, R. L., Zhang, Z. F., Gold,  
18 A., Onasch, T. B., Jayne, J. T., Worsnop, D. R., Gaston, C. J., Thornton, J. A., Vizuete, W.,  
19 Ault, A. P., and Surratt, J. D.: Effect of the aerosol-phase state on secondary organic aerosol  
20 formation from the reactive uptake of isoprene-derived epoxydiols (IEPDX), *Environ. Sci.*  
21 *Tech. Lett.*, 5, 167-174, 10.1021/acs.estlett.8b00044, 2018.

22 Zhang, Y., Sanchez, M. S., Douet, C., Wang, Y., Bateman, A. P., Gong, Z., Kuwata, M.,  
23 Renbaum-Wolff, L., Sato, B. B., Liu, P. F., Bertram, A. K., Geiger, F. M., and Martin, S.  
24 T.: Changing shapes and implied viscosities of suspended submicron particles, *Atmos.*  
25 *Chem. Phys.*, 15, 7819-7829, 10.5194/acp-15-7819-2015, 2015.

26 Zhou, S. M., Shiraiwa, M., McWhinney, R. D., Poschl, U., and Abbatt, J. P. D.: Kinetic  
27 limitations in gas-particle reactions arising from slow diffusion in secondary organic  
28 aerosol, *Faraday Discuss.*, 165, 391-406, <https://doi.10.1039/C3fd00030c>, 2013.

29 Zobrist, B., Marcolli, C., Pedernera, D. A., and Koop, T.: Do atmospheric aerosols form  
30 glasses?, *Atmos. Chem. Phys.*, 8, 5221-5244, 2008.

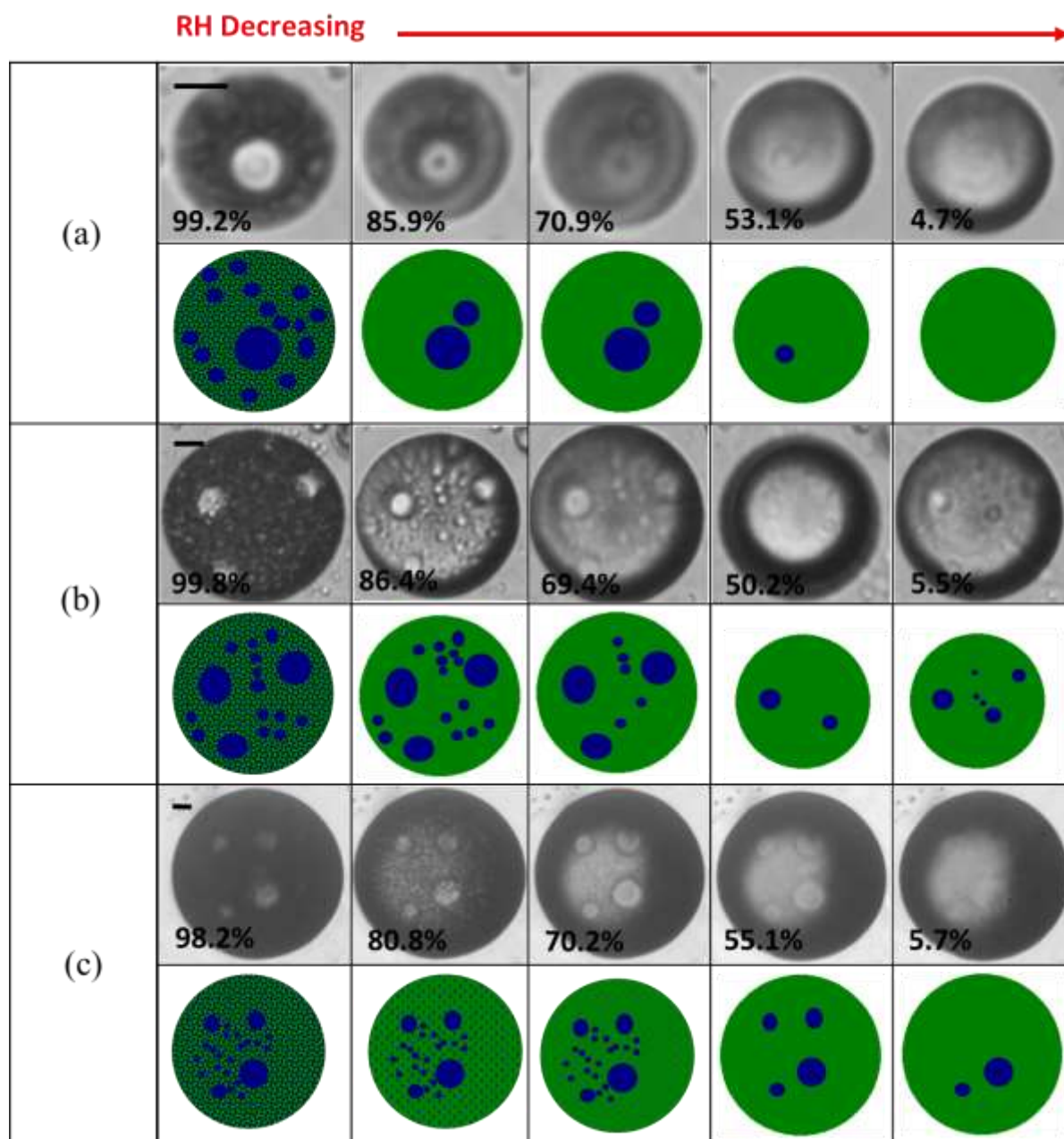
31 Zuend, A. and Seinfeld, J. H.: Modeling the gas-particle partitioning of secondary organic  
32 aerosol: the importance of liquid-liquid phase separation, *Atmos. Chem. Phys.*, 12, 3857–

1 3882, <https://doi.org/10.5194/acp-12-3857-2012>, 2012.

2 Zuend, A., Marcolli, C., Peter, T., and Seinfeld, J. H.: Computation of liquid-liquid equilibria  
3 and phase stabilities: implications for RH-dependent gas/particle partitioning of organic  
4 inorganic aerosols, *Atmos. Chem. Phys.*, 10, 7795–7820, [https://doi.org/10.5194/acp-10-](https://doi.org/10.5194/acp-10-7795-2010)  
5 [7795-2010](https://doi.org/10.5194/acp-10-7795-2010), 2010.

6





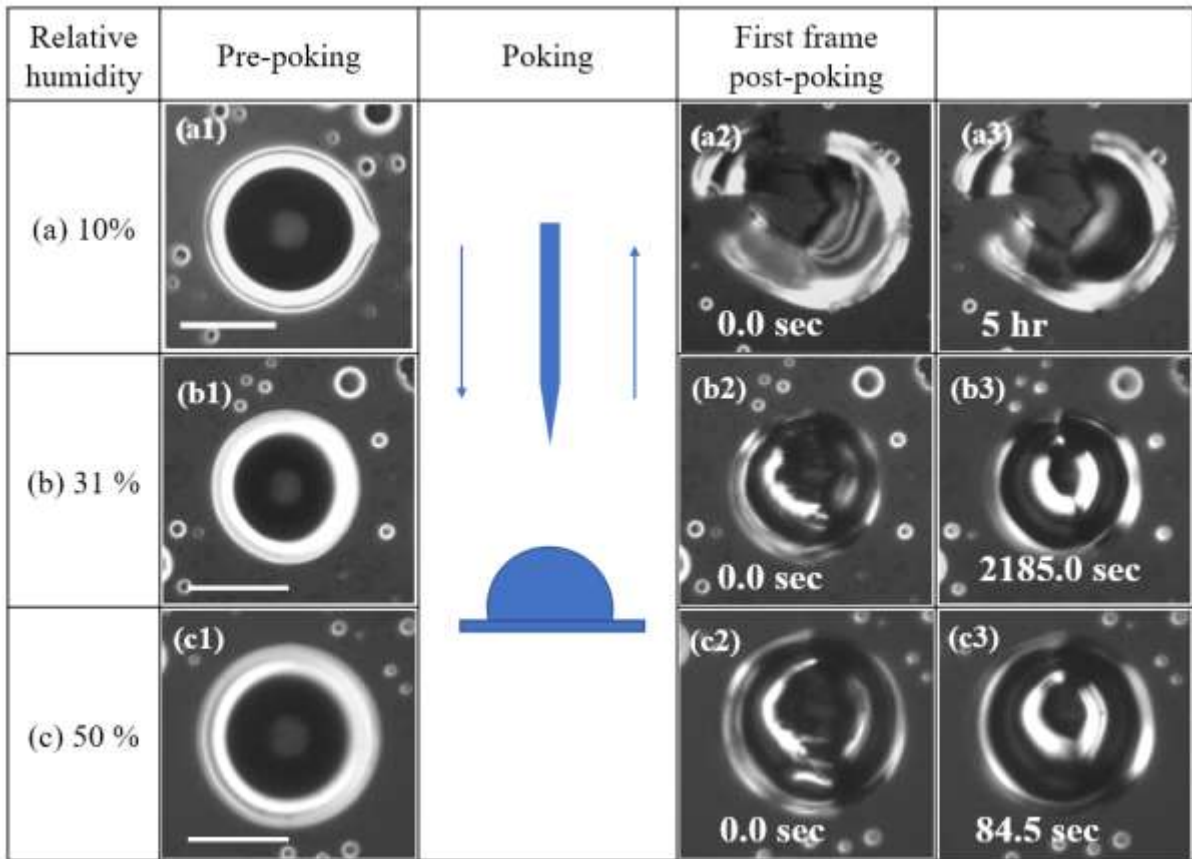
1

2

3 Figure 1. Optical images and illustrations of three diesel fuel SOA particles taken while the RH  
 4 was decreased. Illustrations are provided to help interpret the optical images with green color  
 5 representing the organic-rich phase, and blue color representing the water-rich phase. The  
 6 numbers under the optical images indicate the RH. The length of the scale bar is 10  $\mu\text{m}$ .

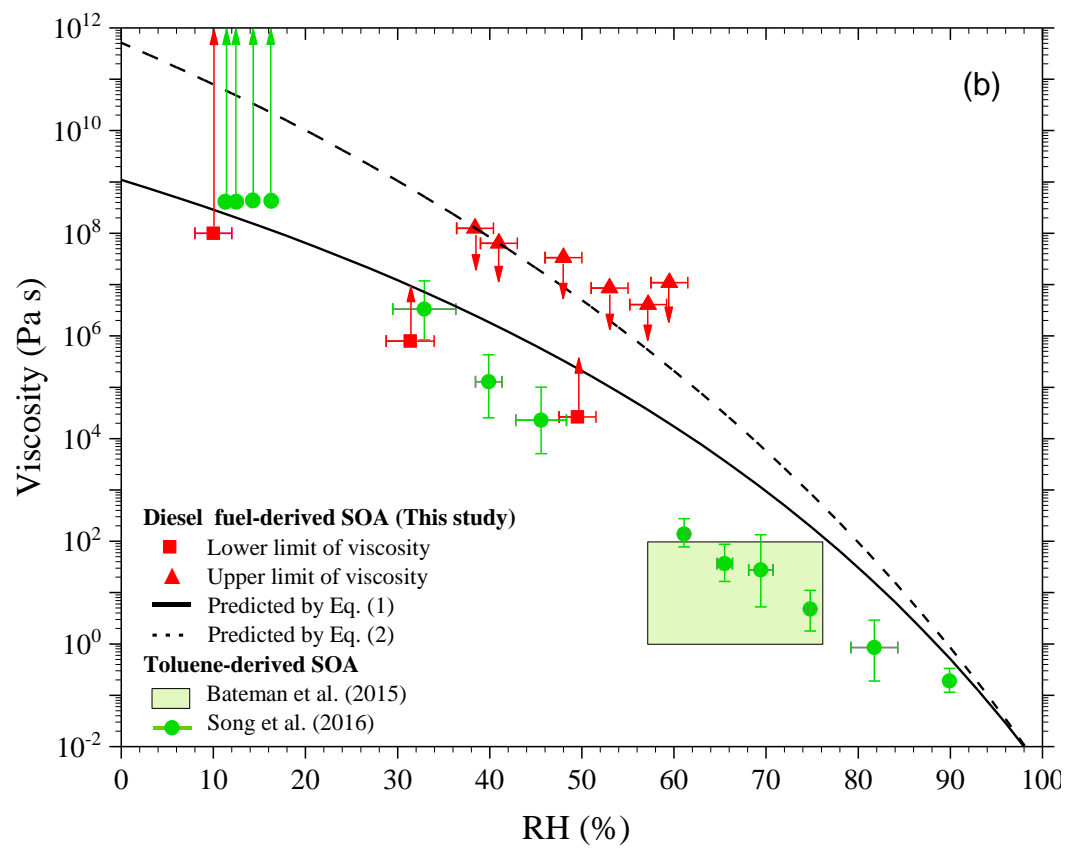
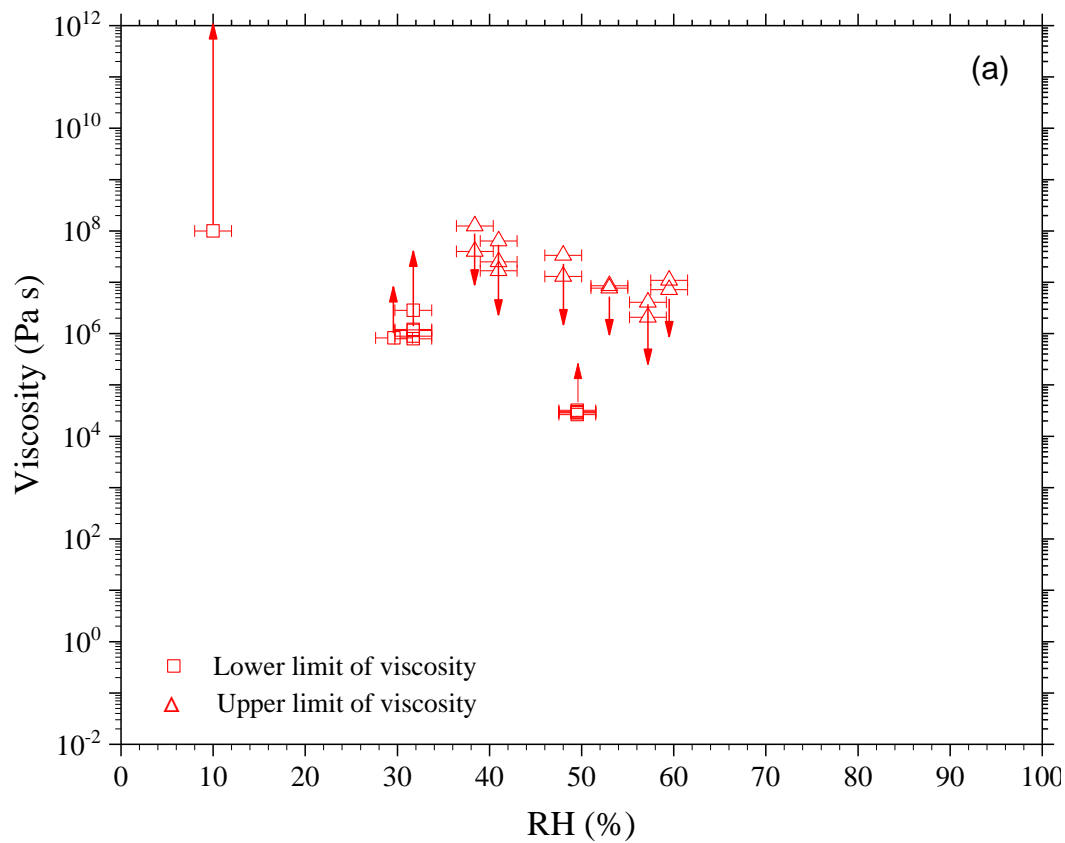
7

8



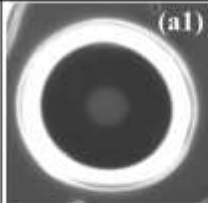
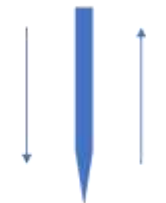
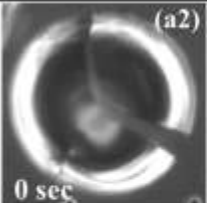
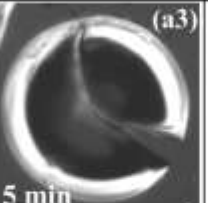
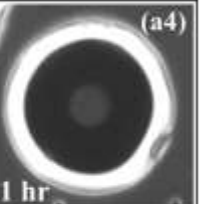
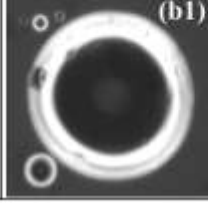

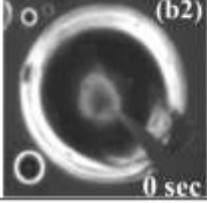
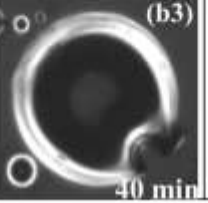
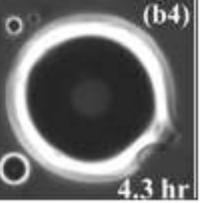
1  
2  
3  
4  
5  
6  
7

Figure 2. Optical images of SOA particles during a poke-and-flow experiment: (a) 10 % RH, (b) 31 % RH, and (c) 50 % RH. The size of the scale bar is 20  $\mu\text{m}$ .



1  
2  
3  
4  
5  
6  
7  
8  
9  
10  
11  
12  
13  
14

Figure 3. (a) Viscosities of diesel fuel SOA. Each data point corresponds to a viscosity determined from poking a single and different particle. Each particle was prepared with the same reaction conditions. Upward arrows indicate lower limit to the viscosities and downward arrows indicate upper limit to the viscosities of diesel fuel SOA. The  $x$  error bars represent uncertainty in the RH measurements. (b) Viscosities of diesel fuel-derived SOA but with the viscosities from individual poke-and-flow experiments grouped by RH. The lower limit to the viscosities and the upper limit to the viscosities represent the lowest and the highest viscosities in the group, respectively. At least two data points were included in each group. The  $x$  error bars represent the lowest and highest RH ranges in the group and the uncertainty in the RH measurements. Also included are viscosities of toluene SOA from Bateman et al. (2015) (green box) and Song et al. (2016) (green circle) and predicted viscosities of the diesel fuel SOA using Eq. (1) (black solid line) and Eq. (2) (black dashed line).

Relative humidity	Pre-poking	Poking	First frame post-poking	During recovery	$\tau_{exp, recovery}$
(a) 53%					
(b) 38 %					

1

2

3 Figure 4. Optical images of diesel fuel SOA particles during poke-and-flow experiments. In  
 4 these experiments the SOA particles were poked at 0 % RH and then exposed to RH values of  
 5 53% (a) and 38% (b). The last column shows the particles after they have returned to a spherical  
 6 cap shape.

7

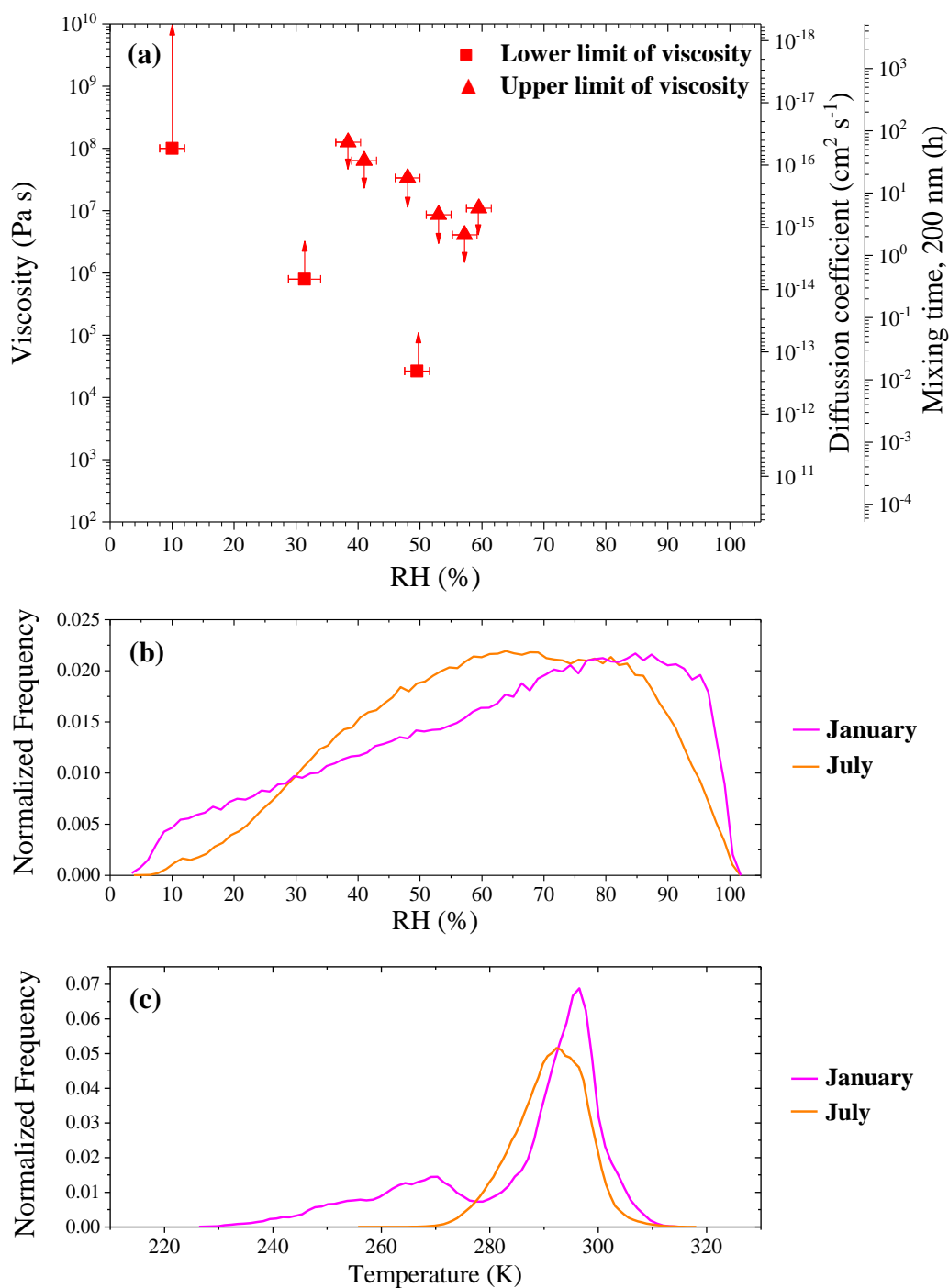
8

9

10

11

12



1  
2

3 Figure 5. Panel (a): Viscosities, diffusion coefficients, and mixing times of organic molecules  
4 within 200 nm diesel fuel SOA. Panel b and c represent the RH frequency distribution and the  
5 temperature frequency distribution in the planetary boundary layer when the average  
6 concentrations of organic aerosol are higher than  $0.5 \mu\text{g m}^{-3}$  at the surface based on GEOS-  
7 Chem (Ullmann et al., 2018). The frequency distributions were calculated using monthly mean

1 meteorological data from GEOS-Chem version v10-01 and data was only included when the  
2 monthly mean concentrations of organic aerosol at the surface were greater than  $0.5 \mu\text{g m}^{-3}$   
3 (Maclean et al., 2017).